



PACIFIC EARTHQUAKE ENGINEERING RESEARCH CENTER

Quantifying Economic Losses from Travel Forgone Following a Large Metropolitan Earthquake

James E. Moore II

University of Southern California

Sungbin Cho

ImageCat, Inc.

Long Beach, California,

and

University of Southern California

Yue Yue Fan

University of California, Davis

and

Stuart Werner

Seismic Systems and Engineering Consultants

Oakland, California

Quantifying Economic Losses from Travel Forgone Following a Large Metropolitan Earthquake

James E. Moore, II

Professor and Chair

Daniel J. Epstein Department of Industrial and Systems Engineering
University of Southern California

Sungbin Cho

ImageCat, Inc.™, Long Beach
and

School of Policy, Planning & Development
University of Southern California

Yue Yue Fan

Assistant Professor

Department of Civil and Environmental Engineering
University of California, Davis

Stuart Werner

Seismic Systems and Engineering Consultants
Oakland

PEER Report 2006/09
Pacific Earthquake Engineering Research Center
College of Engineering
University of California, Berkeley

November 2006

ABSTRACT

The goal of this research is to provide tools for seismic retrofit decisions in metropolitan transportation networks. The objective is to extend the work completed for the PEER Highway Demonstration Project by developing and implementing a transportation network model capable of estimating increased travel delays and the economic losses associated with trips eliminated from the transportation network following an earthquake.

The work completed in PEER projects A5, 104199, and 3222001 links earthquake damage to transportation structures to transportation network performance and traveler responses at a metropolitan scale. Our new results build on this previous work and fit usefully into the FHWA/MCEER REDARS (Risks from Earthquake Damage to Roadway Systems) 2.0 Project. Once fully implemented, REDARS will make an attractive tool for investigating decision support problems of interest to PEER, e.g., evaluating the economic impact of improved bridge performance and/or the ability to more accurately predict performance through improved fragility models.

ACKNOWLEDGMENTS

This work was supported primarily by the Earthquake Engineering Research Centers Program of the National Science Foundation under award number EEC-9701568 through the Pacific Earthquake Engineering Research Center (PEER).

This work made use of the Earthquake Engineering Research Centers Shared Facilities supported by the National Science Foundation under award number EEC-9701471 and by the Federal Highway Administration through the Multidisciplinary Center for Earthquake Engineering Research (MCEER).

Any opinions, findings, and conclusions or recommendations expressed in this material are those of the author(s) and do not necessarily reflect those of the National Science Foundation or the Federal Highway Administration.

CONTENTS

ABSTRACT		iii
ACKNOWLEDGMENTS		iv
TABLE OF CONTENTS		v
LIST OF FIGURES		vii
LIST OF TABLES		ix
1 INTRODUCTION		1
1.1	Modeling Variable Demand for Transportation in Seismic Risk Analysis	1
1.2	Objectives, and Report Structure	4
2 THEORETICAL BACKGROUND OF VARIABLE-DEMAND MODEL		7
2.1	User-Equilibrium Model with Fixed Origin-Destination Demand	7
2.2	Economic Behavior in Transportation Systems	9
2.3	Extending the Fixed-Demand User-Equilibrium Model to Treat Variable-Demand	13
3 NUMERICAL EXAMPLE: COMPUTING BASELINE TRANSPORTATION FLOWS		17
3.1	Data	17
3.2	Solution Steps	19
3.2.1	Iteration 1	19
3.2.2	Iteration 2	22
3.2.3	Iteration 3	24
3.3	Validating Equilibrium Conditions	26
4 APPLICATIONS TO A DAMAGED TRANSPORTATION NETWORK		33
4.1	Scenario 1— Sever Link L_2	33
4.2	Scenario 2— Sever Link L_4	38
4.3	Calculating the Transportation Impacts of an Earthquake Given Variable Demand	44
4.3.1	Case 1: $d_1 = D(t_1)$, $d_2 = D(t_2)$, $d_1 > d_2$, and $t_1 < t_2$	45
4.3.2	Case 2: $d_1 = D(t_1)$, $d_2 = D(t_2)$, $d_1 < d_2$, and $t_1 > t_2$	45
4.3.3	Case 3: $d_1 \neq D(t_1)$	45
4.3.4	Case 4: $d_2 \neq D(t_2)$	45

5	APPLYING VARIABLE-DEMAND MODEL TO REALISTIC EARTHQUAKE IMPACT CALCULATION	47
5.1	Overview of REDARS (<u>R</u> isk from <u>E</u> arthquake <u>D</u> amage to <u>R</u> oadway <u>S</u> ystems	48
5.1.1	Features of REDARS Seismic Risk Analysis	48
5.1.2	REDARS Applications	51
5.2	Bay Area Transportation Data	51
5.3	Hayward Fault Scenario Earthquake	52
5.3.1	Modeling Network Performance and Economic Travel Choices	54
5.3.2	Economic Impacts: Accounting for Value of Forgone Trips	56
6	SUMMARY AND RECOMMENDATIONS FOR FUTURE RESEARCH	59
6.1	Performance of the Algorithm	59
6.2	Demand Shifts versus Variable Demand for Transportation	60
6.3	Network Design	61
6.3.1	Design Problem Complexity	62
6.3.2	Alternative Performance Metrics	63
6.3.3	Role of Heuristics	64
	REFERENCES	65

LIST OF FIGURES

Figure 1.1	Cumulative distribution of post-earthquake volume/capacity ratios: comparison of fixed and variable travel-demand estimates	3
Figure 2.1	Network equilibrium conditions given constant travel demand.....	9
Figure 2.2	Effect of earthquake on total travel time given constant travel demand	10
Figure 2.3	Effect of an earthquake given variable travel demand	12
Figure 3.1	Network configuration for numerical example	18
Figure 3.2	Link travel times and volumes (passenger car equivalents) after 30 iterations.....	29
Figure 4.1	Network configuration for scenario 1 — sever link L_2	34
Figure 4.2	Travel demands and travel times: baseline vs. scenario 1	37
Figure 4.3	Adjusting \bar{q}_{24}^2 to achieve a feasible solution describing baseline conditions.....	38
Figure 4.4	Network configuration for scenario 2 — sever link L_4	39
Figure 4.5	Travel demands and travel times: baseline vs. scenario 2	43
Figure 4.6	Adjust D_{24}^2 to achieve a feasible solution describing baseline conditions and scenario 2 results	44
Figure 5.1	REDARS methodology for seismic risk analysis of highway systems.....	49
Figure 5.2	REDARS SRA modules	50
Figure 5.3	San Francisco Bay Area roadway network characterized by REDARS 2.0 import wizard	53
Figure 5.4	Observed and estimated San Francisco Bay Area baseline interzonal trip rates as a function of travel time	54
Figure 5.5	Bridge and link damage states associated with Hayward fault scenario earthquake.....	55
Figure 5.6	VDM is most effective at accounting for elasticity of travel between zone pairs subject to intense travel demands	56
Figure 5.7	Total household transportation impacts associated with Hayward fault scenario earthquake.....	58
Figure 6.1	Movement along demand curve versus shift in demand: light hatched areas represent economic losses to remaining and absent travelers	61

LIST OF TABLES

Table 3.1	Maximum demands between zone pairs.....	18
Table 3.2a	Link volumes initialized at zero	19
Table 3.2b	Travel demands initialized at zero.....	19
Table 3.3	Link travel times initialized at free-flow travel times	19
Table 3.4	Initializing auxiliary demands as maximum demands	20
Table 3.5	Initializing auxiliary link volumes: loading shortest paths.....	20
Table 3.6	Updating initial zero travel demand to auxiliary travel demand	21
Table 3.7	Updating initial zero link flows to auxiliary link flows	21
Table 3.8	Updating link travel times in response to updated link flows	22
Table 3.9	Updating auxiliary travel demands in response to link travel times	22
Table 3.10	Updating auxiliary link volumes: loading shortest paths	23
Table 3.11	Updating travel demand, $\alpha = 0.5256$	23
Table 3.12	Updating link volumes, $\alpha = 0.5256$	23
Table 3.13	Updating link travel times in response to updated link flows	24
Table 3.14	Updating auxiliary travel demands in response to link travel times	24
Table 3.15	Updating auxiliary link volumes: loading shortest paths	25
Table 3.16	Updating travel demand, $\alpha = 0.1647$	25
Table 3.17	Updating link volumes, $\alpha = 0.1647$	25
Table 3.18	Travel demands and shortest path times for baseline example of variable-demand model: iterations 1–30	27
Table 3.19	Link volumes and link travel times for numerical example of variable-demand model: iterations 1–30	28
Table 3.20	Comparison of travel times on competing paths	29
Table 3.21	Comparison of travel demands, VDM and travel-demand function values	30
Table 4.1	Travel demands and shortest path times for scenario 1: iterations 1–30.....	35
Table 4.2	Changes in travel demands and travel times: baseline vs. scenario 1	36
Table 4.3	Impacts associated with scenario 1 (passenger car equivalent minutes).....	39
Table 4.4	Travel demands and shortest path times for scenario 2: iterations 1–30.....	40
Table 4.5	Changes in travel demands and travel times: baseline vs. scenario 2	41

Table 4.6 Impacts associated with scenario 2 (passenger car equivalent minutes).....42

Table 5.1 Bay Area transportation impacts of Hayward fault scenario earthquake57

1 Introduction

1.1 MODELING VARIABLE DEMAND FOR TRANSPORTATION IN SEISMIC RISK ANALYSIS

A user-equilibrium network analysis model is widely used in transportation analysis to model the network level of service as a function of network topology and demand for transportation. This standard transportation planning model was also included in the beta version of REDARS (Risks from Earthquake Damage to Roadway Systems) as a proof of the concept.

However, a validation study of REDARS showed that the model substantially overestimated travel volumes and times in the Los Angeles network relative to observations following the 1994 Northridge earthquake in Los Angeles. In some cases, the model overestimation of volumes was up to 2.5 times greater than observed on the day following the earthquake, and of delays up to 12 times greater than observed (Cho et al. 2003a; Werner et al. 2004). These results suggest that the standard version of the user-equilibrium network model is of limited use for seismic risk analysis, since it is not able to reproduce stable travel increments even immediately after a major earthquake affecting the highway system. The observed changes in total delay are much smaller than predicted.

From an economic perspective, the reductions in network capacity produce a reduction in level of service that in turn produces an attendant reduction in demand for transportation services. The impact of the Northridge earthquake on the Los Angeles freeway system resulted in several major freeways out of service. The network abruptly experienced an unparalleled reduction in capacity. If travel demand had remained unchanged, this abrupt reduction in network supply would necessarily have led to an enormous increase in the equilibrium cost of travel, i.e., travel time. In the case of the Northridge earthquake, this increase was never realized.

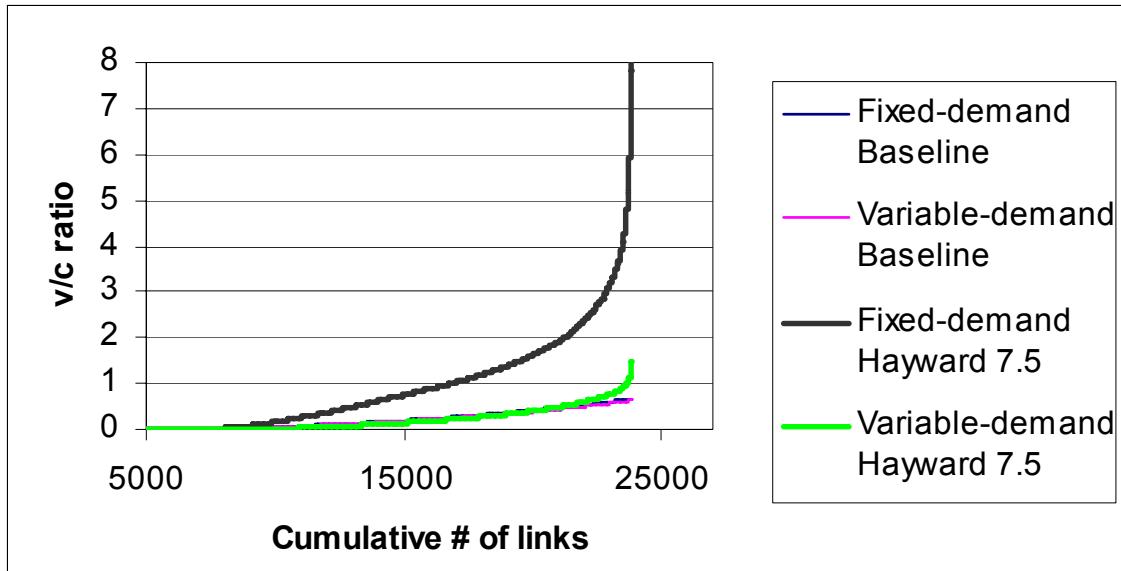
The 1994 Northridge earthquake is perhaps the best documented earthquake in the United States. A considerable amount of data relating to transportation impacts is available. The reports generated from the data help to understand changes in travel patterns resulting from the large-scale network disruption produced by the earthquake. Four months of close observation, including household surveys, transit rider surveys, and freight surveys, indicate a substantial overall travel-time increment.

Local traffic volumes on some links near collapsed bridge sites (Interstate 10/La Cienega, State Route 118/Gothic, and Interstate 5/State Route 14) were double the pre-earthquake volumes on the very day after the earthquake. The nonlinear relationship between traffic volumes and delays means that this increase in volume would more than double travel times on some links. More generally, during the recovery period, the travel-time increment resulting from reduced capacity was not more than 15 minutes per trip relative to pre-quake conditions.

Similar theoretical results were documented in the initial work done as part of the Pacific Earthquake Engineering Research (PEER) Center's multi-year Highway Demonstration Project (Kiremidjian et al. 2006). Initial efforts to model changes in travel patterns and traffic delays associated with large Bay Area scenario earthquakes on the San Andreas and Hayward faults consistently produced unfeasibly large flows and unrealistically high delays on network links.

It is important that transportation network models applied to seismic risk analysis have a capacity to endogenize travel demand in response to changes in the network level of service (Cho et al. 2003b). These changes result from interactions between travel demand and network capacity. The objective is to model equilibrium travel flows on a network in which changes in capacity induce simultaneous and consistent changes in level of service and travel demand. This is an extension of the standard user-equilibrium network model to include variable demand, hereafter called the "variable demand model (VDM)." From an economic perspective, this reformulation might most appropriately be labeled an "elastic demand model," but since "VDM" has been promulgated in research published by PEER and the Multidisciplinary Center for Earthquake Engineering Research (MCEER), its usage is continued here.

An initial formulation of a VDM for analysis of transportation networks subject to seismic risk was published in the report for the PEER Highway Demonstration Project (Kiremidjian et al. 2006). These initial results are encouraging, producing nearly feasible transportation flows in all circumstances (Fig. 1.1). Link volume/capacity ratios in excess of 1.0



Source: Kiremidjian et al. (2006) *Pacific Earthquake Engineering Research Center Highway Demonstration Project* PEER Report 2006/02.

Fig. 1.1 Cumulative distribution of post-earthquake volume/capacity ratios: comparison of fixed and variable travel-demand estimates

represent unfeasibly large flows. Unfortunately, such results are routinely predicted if post-earthquake travel demands are fixed at pre-earthquake levels. A variable-demand model can replicate the same baseline, pre-event conditions as a standard fixed-demand formulation and predicts nearly feasible flows following the scenario earthquake, in this case a moment magnitude 7.5 event occurring on the Hayward fault.

The application of a VDM to seismic risk analysis also permits a more sophisticated accounting of the social cost of damage to the transportation network resulting from an earthquake. The standard transportation planning perspective is that the difference in total travel time accruing on the network, calculated by summing the travel time of each user across all users, before and after an earthquake is society's transportation *cost* of the earthquake. This simple concept is inadequate if losses in capacity are significant enough to produce changes in the level of service large enough to diminish travel demand. A VDM application reduces travel demand, which leads to more moderate changes of travel time. As a result, the total travel time accruing on a network subject to earthquake damage may be less than the total travel time accruing before the earthquake. If attention is restricted to aggregate travel time, then earthquakes might appear to be a source of social benefits. They are not. Meaningfully applying

a VDM to seismic risk analysis requires a new means for accounting for the social costs resulting from transportation impacts.

1.2 OBJECTIVES, AND REPORT STRUCTURE

This study provides a method for calculating the social cost resulting from earthquake damage to transportation networks. This approach is based on use of an improved VDM to estimate zone-to-zone changes in travel demand and travel times. Reductions in capacity cause increases in travel times and decreases in travel demand. However, in applications to actual network systems, earthquake damage may increase the capacity available for service between some zone-pairs by eliminating competing access to these facilities. As a result, in some highly localized portions of the network, the level of service may genuinely improve following an earthquake.

Accounting for the economic behavior of travelers requires that travel-demand curves be parameterized and estimated. Once this step is taken, the information in these demand curves can be further leveraged to compute the value of trips that are no longer occurring due to reductions in network level of service, i.e., the value of forgone travel.

An examination of the results generated for the PEER Highway Demonstration Project, and an attempt to incorporate this modeling capability into REDARS revealed that previous attempts to implement the model had led to incomplete numerical convergence. The travel-demand relationships associated with large flows between traffic analysis zone (TAZ) pairs were always treated correctly, but the results for many zone pairs with small interzonal flows deviated from the travel-demand functions built into the VDM. These results persisted despite the fact that the algorithm implemented to solve the large-scale VDM appeared to have converged.

A simple example is used to demonstrate how the VDM estimates demand reductions while identifying network equilibrium flows. The example also exhibits some counterintuitive outcomes affecting the calculation of social costs. Chapter 2 provides theoretical background for the user-equilibrium network model, and gives the VDM as an extension of the standard user-equilibrium model. Chapter 2 also includes solution algorithms for the two models, including an improved algorithm for the VDM, and the general framework for calculating social costs based on model outputs.

A simple example network is used in Chapter 3 to provide detailed calculation steps for the VDM solution algorithm. In Chapter 4, two damage scenarios are applied to a simple

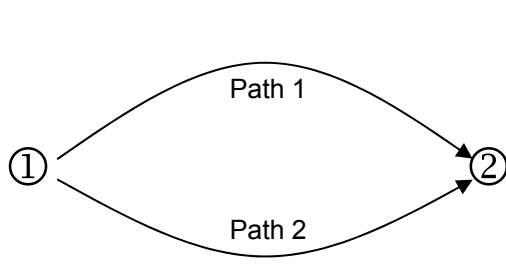
example network, and the social cost is calculated for each case by examining flows between each zone pair. Chapter 5 summarizes REDARS, applies the VDM implementation in REDARS to a more realistic scenario, and performs social cost calculations by the method described in Chapter 4. A summary and recommendations for future research are provided in Chapter 6.

2 Theoretical Background of Variable-Demand Model

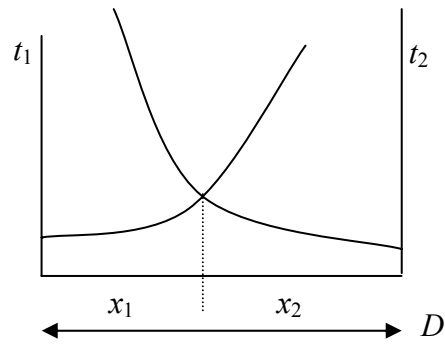
2.1 USER-EQUILIBRIUM MODEL WITH FIXED ORIGIN-DESTINATION DEMAND

Static transportation network models are based on Wardrop's rules of network equilibrium (Wardrop 1952, recited from Sheffi 1985). According to these rules, the travel times along the *used* paths between any origin-destination pair in a network are identical and less than the travel times on *unused* paths. As a result, individual drivers cannot improve their driving times by altering their routes, and are in an equilibrium state. The standard user-equilibrium model computes travel time and link volumes that are consistent with Wardrop's rules. This is nontrivial because links are congested, and travel times vary with link flows. Because paths overlap and share links, each traveler's choice of path affects the costs of options available to others. Based on the conceptual model formulated by Beckmann et al. (1956), Frank and Wolfe (1956) developed an efficient solution algorithm that can be applied to large-scale transportation networks.

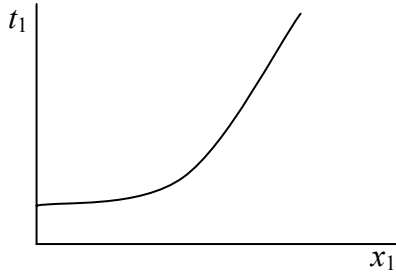
A simple transportation network is used to derive the mathematical formulation for the network equilibrium problem (Fig. 2.1). A total of D drivers will travel from Zone 1 to Zone 2 by using either of the two paths 1 and 2, as shown in Figure 2.1(a). Let x_i and t_i be the traffic volume and travel time on paths $i = 1, 2$, respectively. Travel time t_i is a convex function of traffic volume, and this convexity represents congestion. Figures 2.1(c) and (d) are the assumed graphical forms for the congestion functions on paths 1 and 2, respectively. If drivers are perfectly rational and perfectly informed, then travel times on both paths should be identical in an equilibrium state, as in Figure 2.1(b). Otherwise more drivers would take the path with shorter travel time. In this figure, the total number of drivers D is the sum of x_1 and x_2 . The



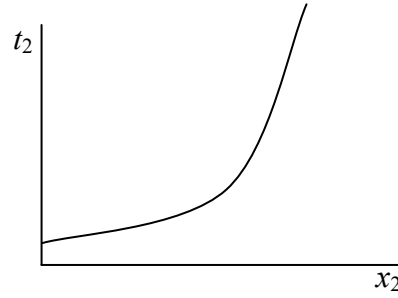
(a) Network configuration



(b) Equilibrium conditions



(c) Congestion function for path 1



(d) Congestion function for path 2

Fig. 2.1 Network equilibrium conditions given constant travel demand

combined area below the two congestion functions depicted in Figure 2.1(b) is minimized for given travel demand D when the travel times t_1 and t_2 are equalized. This minimization of the sum of the congestion function integrals is formulated as the following constrained optimization problem. This is the standard representation of the user-equilibrium flow model.

$$\min z(\mathbf{x}) = \sum_a \int_0^{x_a} t_a(w) dw \quad (2.1)$$

subject to

$$\sum_k f_k^{rs} = q_{rs} \quad \forall r, s \quad (2.2)$$

$$f_k^{rs} \geq 0 \quad \forall k, r, s \quad (2.3)$$

$$q_{rs} \geq 0 \quad \forall r, s \quad (2.4)$$

$$x_a = \sum_{rs} \sum_k f_k^{rs} \cdot \delta_{a,k}^{rs} \quad \forall a \quad (2.5)$$

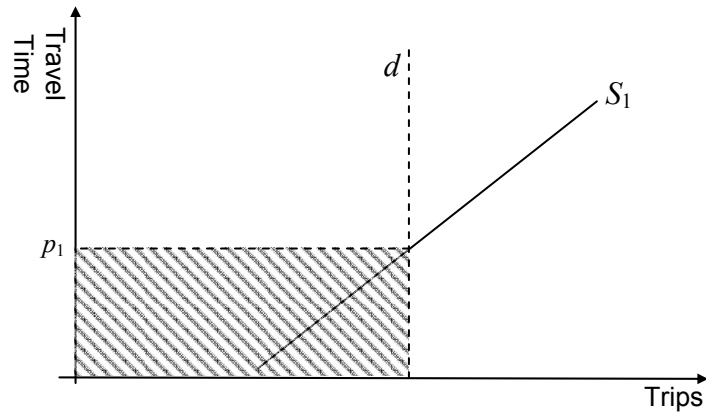
where

- t_a : link performance function of link a .
- f_k^{rs} : flow on path k connecting OD (origin-destination) pair r - s .
- q_{rs} : travel demand between OD pair r - s .
- x_a : flow on link a .
- $\delta_{a,k}^{rs}$: 1 if link a is on path k between OD pair r - s , otherwise 0.

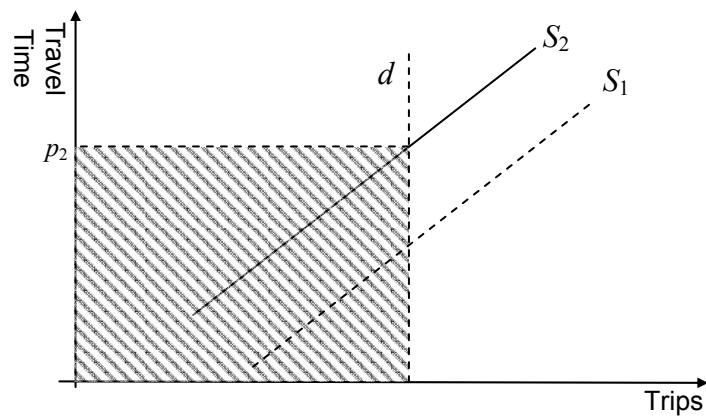
2.2 ECONOMIC BEHAVIOR IN TRANSPORTATION SYSTEMS

The user-equilibrium model has been successfully applied to problems such as evaluating alternative transportation projects to provide additional network capacity in response to increasing population or propensity to travel. Most metropolitan planning applications rely on an implementation of this static (time-independent) model. However, in seismic risk analysis, the network is at risk of losing significant capacity. The resulting changes in the level of service produce reductions in travel demand, and the fixed-demand assumption associated with the standard user-equilibrium model will overestimate the total delays associated with post-earthquake travel conditions.

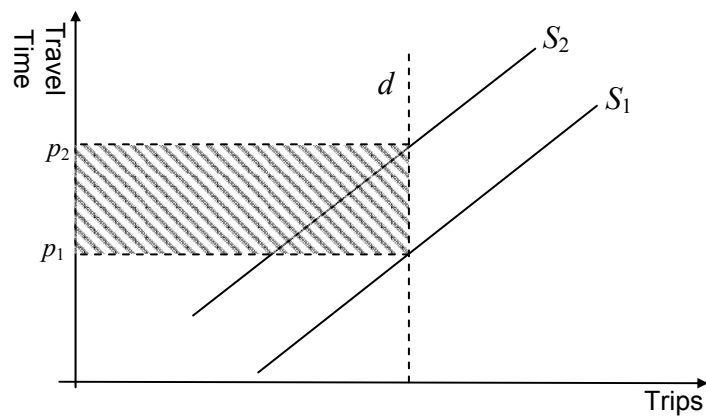
Figure 2.2 depicts the effect of an earthquake on the transportation system if the demand for travel is fixed, assuming drivers have sufficient information to select rational paths following the event. If an earthquake damages the links in the transportation network, the supply curve shifts in the upwards-left direction. Network capacity is reduced from supply curve S_1 in Figure 2.2(a) to S_2 in Figure 2.2(b), while the demand remains constant at d . The corresponding travel time, i.e., the equilibrium travel cost, shifts from p_1 in Figure 2.2(a) to p_2 in Figure 2.2(b). The shaded areas in Figures 2.2(a) and(b) represent the total travel times that drivers experience in the aggregate in the pre- and post-earthquake networks, respectively. The difference, shaded in Figure 2.2(c), represents the overstated travel-time impacts resulting from earthquake damage to the transportation network.



(a) Pre-earthquake equilibrium travel times and volumes given constant travel demand



(b) Post-earthquake equilibrium travel times and volumes given constant travel demand



(c) Increase in total travel times given constant travel demand

Fig. 2.2 Effect of earthquake on total travel time given constant travel demand

However, travelers' decisions are not restricted to the choice of route. These decisions also include choice of destination and whether to make a trip. Travel is a derived demand. The cost of travel, delay included, is the cost of whatever the trip makes possible. In a highly congested roadway network, any rational driver who expects the value of travel time to exceed the expected benefit derived from the trip will decline to travel.

Figure 2.3 shows the effect of the elastic (variable) demand on the level of service and net benefits provided by a transportation system subjected to damage from an earthquake. Before the earthquake occurs, the transportation system performs according to supply curve S_1 . Travel-demand curve D interacts with the supply to define equilibrium trip level d_1 and equilibrium travel cost p_1 .

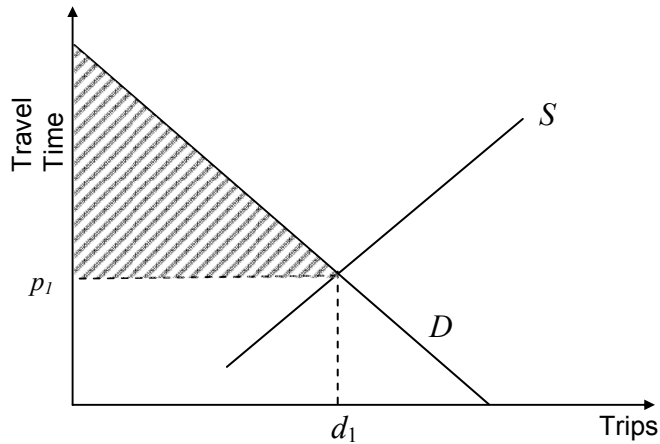
The demand curve D represents the number of drivers willing to travel as a function of travel time. This travel-demand curve is also interpreted as the *willingness to pay* (in terms of time) to obtain transportation services. Prior to the earthquake, d_1 trips are being taken by travelers who have a willingness to pay that exceeds the equilibrium travel cost p_1 . The shaded triangle in Figure 2.3(a) characterizes aggregate net benefits incurred by drivers' making trips. This is a measure of *consumer surplus* in the transportation system. No more than d_1 trips occur because the equilibrium travel cost p_1 exceeds the willingness to pay on the part of all individuals who choose not to travel.

If earthquake damage occurs to the links in the transportation network, the supply curve again shifts in the upwards-left direction. The equilibrium travel cost is relative to the pre-earthquake levels condition for the same demand, and fewer trips are take place. Figure 2.3(b) depicts this situation. A total of d_2 travelers exhibit a willingness to pay that exceeds the equilibrium travel cost p_2 . The following inequalities hold:

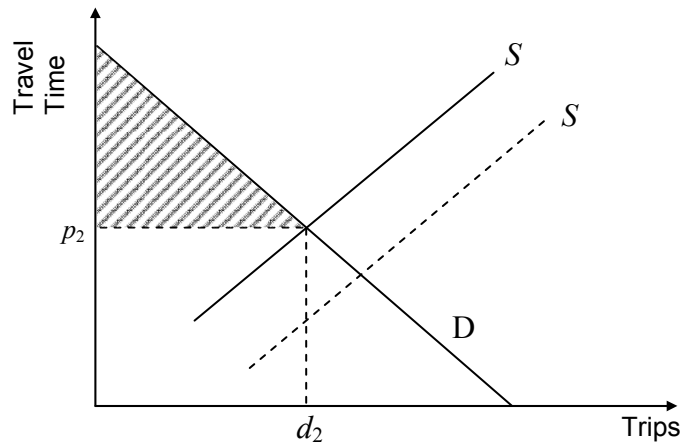
$$d_2 \leq d_1, \text{ and} \tag{2.6}$$

$$p_1 \leq p_2. \tag{2.7}$$

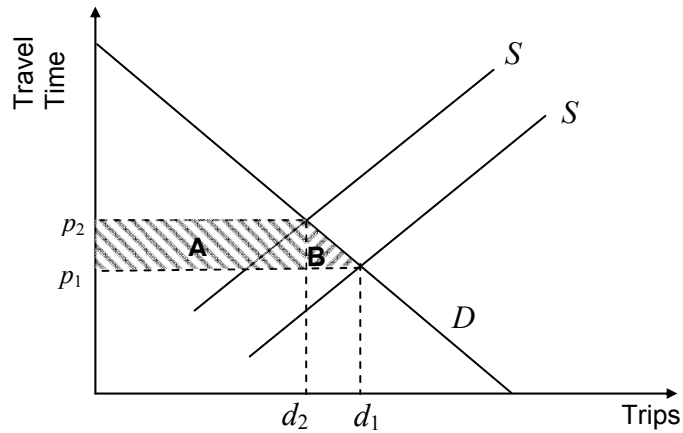
Typically, though not inevitably, earthquakes reduce the consumer surplus accruing to travelers by reducing network capacity. Figure 2.3(c) summarizes the effect of an earthquake. The shaded trapezoid in Figure 2.3(c) represents the total loss in benefits that results from the earthquake. The loss can be divided into two parts. The shaded rectangle labeled A, the area of which can be calculated as $[p_2 - p_1] \times d_2$, is the additional total travel time experienced by the drivers who remain in the earthquake-damaged system. The shaded triangle labeled B is the loss



(a) Pre-earthquake travel demand–supply equilibrium and consumer surplus given variable travel demand



(b) Post-earthquake travel demand–supply equilibrium and consumer surplus given variable travel demand



(c) Changes in the travel demand–supply equilibrium and consumer surplus given variable travel demand

Fig. 2.3 Effect of earthquake given variable travel demand

associated with trips forgone. Calculating these losses requires equilibrium travel time and trip estimates that account for variable travel demand.

2.3 EXTENDING THE FIXED-DEMAND USER-EQUILIBRIUM MODEL TO TREAT VARIABLE DEMAND

The problem addressed by a user-equilibrium model with the variable travel-demand model is to find the link volumes, link travel times, and travel-demand levels that simultaneously satisfy the conditions for economic equilibrium on the network and are consistent with travel-demand curves. Wardrop's first principle still holds: At equilibrium, the travel time on all used paths between any origin-destination zone pair are equal, and are also equal to or less than the travel times on any unused paths. In addition, the trip rates (origin-destination requirements) implied by these travel times must satisfy the demand function, which determines the number of travelers whose willingness to pay exceeds the equilibrium travel time between each zone pair. These equilibrium trip rates, in turn, influence travel times because the number of trips loaded onto the network determines zone-to-zone travel times.

These conditions define the user equilibrium with variable demand. Beckmann et al. (1956) formulated the user-equilibrium network problem model with elastic travel demand as an optimization problem. The mathematical form to the model is as follows.

$$\max z(\mathbf{x}, \mathbf{q}) = \sum_a \int_0^{x_a} t_a(w) dw - \sum_{rs} \int_0^{q_{rs}} D_{rs}^{-1}(w) dw \quad (2.8)$$

subject to

$$\sum_k f_k^{rs} = q_{rs} \quad \forall r, s \quad (2.9)$$

$$f_k^{rs} \geq 0 \quad \forall k, r, s \quad (2.10)$$

$$q_{rs} \geq 0 \quad \forall r, s \quad (2.11)$$

$$q_{rs} = D_{rs}(u_{rs}) \quad \forall r, s \quad (2.12)$$

$$x_a = \sum_{rs} \sum_k f_k^{rs} \cdot \delta_{a,k}^{rs} \quad \forall a \quad (2.13)$$

where

t_a : link performance function of link a .

D : demand function.

- D^{-1} : inverse of demand function.
- f_k^{rs} : flow on path k connecting OD pair $r-s$.
- q_{rs} : trip rate between OD pair $r-s$.
- u_{rs} : travel time between OD pair $r-s$.
- x_a : flow on link a .
- $\delta_{a,k}^{rs}$: 1 if link a is on path k between OD pair $r-s$, otherwise 0.

The first term in the objective function ensures that link volumes and travel times conform to user-equilibrium conditions. The second term adjusts trip rates between zone-pairs so that the travel demand loaded onto the network corresponds to travel times.

LeBlanc and Farhangian (1981) provided an efficient solution algorithm for this problem, which follows the general secant method.

Step 0: Initialization

Find an initial feasible flow pattern $\{x_a^n\}, \{q_{rs}^n\}$. Set index $n:=1$.

Step 1: Update link travel times and the times associated with trip making

$$\text{Set } t_a^n = t_a(x_a^n) \forall a. \text{ Compute } D_{rs}^{-1}(q_{rs}^n) \forall r, s. \quad (2.14)$$

Step 2: Find auxiliary link volumes and trip rates

Compute the shortest path, m , between each O-D pair $r-s$ based on link travel time $\{t_a^n\}$.

$$\text{Set } c_m^{rs^n} = \min_{\forall k} \{c_k^{rs^n}(t_a^n)\}. \quad (2.15)$$

Find auxiliary trip rates.

$$\text{If } c_m^{rs^n} < D_{rs}^{-1}(q_{rs}^n), \text{ set } g_m^{rs^n} = \overline{q_{rs}} \quad (2.16)$$

where m is shortest path, and $\overline{q_{rs}}$ is upper bound of the trip rate for travel between pair $r-s$.

$$\text{If } c_m^{rs^n} > D_{rs}^{-1}(q_{rs}^n), \text{ set } g_k^{rs^n} = 0 \forall k. \quad (2.17)$$

$$\text{If } \left| c_m^{rs^n} - D_{rs}^{-1}(q_{rs}^n) \right| < \varepsilon, \text{ set } g_m^{rs^n} = g_m^{rs^{n-1}}. \quad (2.18)$$

$$\text{Auxiliary link volume } y_a^n = \sum_{rs} \sum_k g_k^{rs^n} \cdot \delta_{a,k}^{rs} \forall a. \quad (2.19)$$

$$\text{Auxiliary trip rate } v_{rs}^n = \sum_k g_k^{rs^n} \forall r, s. \quad (2.20)$$

Step 3: Find the best moving step with which to adjust the current set of flows and demands

Solve following system for α .

$$\min z(\alpha) \sum_a \int_0^{x_a^n + \alpha(y_a^n - x_a^n)} t_a(w) dw - \sum_{rs} \int_0^{q_{rs}^n + \alpha(v_{rs}^n - q_{rs}^n)} D_{rs}^{-1}(w) dw \quad (2.21)$$

$$\text{subject to} \quad 0 \leq \alpha \leq 1$$

Step 4: Update travel demands and link flows

$$q_{rs}^{n+1} = q_{rs}^n + \alpha(v_{rs}^n - q_{rs}^n) \quad (2.22)$$

$$x_a^{n+1} = x_a^n + \alpha(y_a^n - x_a^n) \quad (2.23)$$

Step 5: Convergence test

If following inequality holds for very small κ , terminate. Otherwise, set index $n:=n+1$ and go to step 1. (2.24)

$$\sum_{rs} \frac{|D_{rs}^{-1}(q_{rs}^n) - u_{rs}^n|}{u_{rs}^n} + \sum_{rs} \frac{|u_{rs}^n - u_{rs}^{n-1}|}{u_{rs}^n} \leq \kappa \quad (2.25)$$

3 Numerical Example: Computing Baseline Transportation Flows

The VDM is applied to a small synthetic transportation system, and the solution steps are presented in detail. The small size of this example makes it possible to display calculations at every step for all the variables in the system. The results from this example will be used in Chapter 5 in the calculation of social costs.

3.1 DATA

The transportation system in this example includes five links, labeled L_a and four traffic zones labeled Z_r . (See Fig. 3.1.) The transportation network is arranged such that link L_2 is used by all three zone pairs in the system. Trips between zone pairs Z_{14} and Z_{34} might occur across alternative routes L_1 versus $L_4 + L_2$, and L_3 versus $L_5 + L_2$, respectively. Trips between zone pair Z_{24} , are accommodated only on route L_2 . The congestion function for each link L_a is $t_i(x)$, which defines the travel time for a given traffic volume on each link. The BPR (Bureau of Public Road) function is used to account for link congestion. The BPR function includes parameters for effective capacity and free-flow travel time.

$$t_1(x) = 10 \cdot \left(1 + 0.15 \cdot \left[\frac{x}{8} \right]^4 \right), \quad t_2(x) = 7 \cdot \left(1 + 0.15 \cdot \left[\frac{x}{12} \right]^4 \right), \quad (3.1), (3.2)$$

$$t_3(x) = 9 \cdot \left(1 + 0.15 \cdot \left[\frac{x}{6} \right]^4 \right), \quad t_4(x) = 4 \cdot \left(1 + 0.15 \cdot \left[\frac{x}{3} \right]^4 \right), \quad (3.3), (3.4)$$

$$t_5(x) = 4 \cdot \left(1 + 0.15 \cdot \left[\frac{x}{3} \right]^4 \right) \quad (3.5)$$

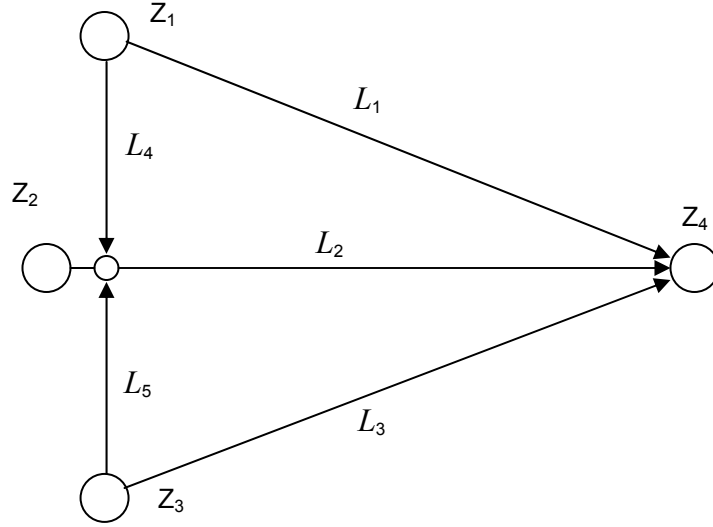


Fig. 3.1 Network configuration for numerical example

Two classes of travel demands originate from each of the first three zones, Z_1 through Z_3 , and are destined for the last zone, Z_4 . The demand for travel between each zone pair is given by a function of the equilibrium travel time between the zone pair $r-s$. The demand function $D_{rs}^k(t_{rs})$ represents the demand for travel by class k between zones $r-s$ given travel time t_{rs} . The negative exponential function is widely used to characterize the way demand for travel decreases as travel time increases.

$$D_{14}^1 = 36.0 \cdot \exp(0.3 - 0.1 \cdot t_{14}) \quad D_{14}^2 = 9.8 \cdot \exp(0.002 - 0.05 \cdot t_{14}) \quad (3.6), (3.7)$$

$$D_{24}^1 = 14.4 \cdot \exp(0.3 - 0.1 \cdot t_{24}) \quad D_{24}^2 = 6.0 \cdot \exp(0.002 - 0.05 \cdot t_{24}) \quad (3.8), (3.9)$$

$$D_{34}^1 = 18.0 \cdot \exp(0.3 - 0.1 \cdot t_{34}) \quad D_{34}^2 = 14.0 \cdot \exp(0.002 - 0.05 \cdot t_{34}) \quad (3.10)$$

The coefficients in each exponential function are unique to each class of trip. These functions are usually calibrated for each observed OD matrix for each trip class against observed travel times. Maximum demands by trip class between all zone pairs $r-s$, \bar{q}_{rs}^k , are required to calculate auxiliary demand. The values for this example appear in Table 3.1.

Table 3.1 Maximum demands between zone pairs

		Z_{14}	Z_{24}	Z_{34}
Demand, \bar{q}_{rs}	Trip Class $k=1$	20.00	9.00	12.00
	Trip Class $k=2$	7.00	4.00	10.00

3.2 SOLUTION STEPS

Based on this input data, the detailed calculation steps from the first three iterations of the LeBlanc and Farhangian algorithm ($n:=1$ to 3) follows.

3.2.1 Iteration 1

Step 0: Initialization

In the initial stage, all the link volumes and demands are set to zero. Set $n:=1$.

Table 3.2a Link volumes initialized at zero

	L_1	L_2	L_3	L_4	L_5
Volume $x_a^{n=1}$	0.00	0.00	0.00	0.00	0.00

Table 3.2b Travel demands initialized at zero

		Z_{14}	Z_{24}	Z_{34}
Demand, $q_{rs}^{n=1}$	Trip Class $k=1$	0.00	0.00	0.00
	Trip Class $k=2$	0.00	0.00	0.00

Step 1: Initializing link travel times

This step applies the current link traffic volumes (0 in iteration 1) to the congestion functions to calculate link travel times. These are free-flow travel times in iteration 1.

Table 3.3 Link travel times initialized at free-flow travel times

	L_1	L_2	L_3	L_4	L_5
Time, $t_a^{n=1} = t_a(x_a^{n=1})$	10.00	7.00	9.00	4.00	4.00

Step 2: Initializing auxiliary travel demands and auxiliary link volumes

Auxiliary demands for each trip class, $v_{rs}^{n=1,k}$, are calculated by comparing the travel time on the shortest path between each OD pair $r-s$ to the inverse of demand functions, $D_{rs}^k^{-1}(\bullet)$ evaluated at the current set of demands, $q_{rs}^{n=1,k}$. These evaluations return another set of time values that correspond to the current demands. If the shortest path travel time is smaller than the time provided by the inverse demand function, the auxiliary demand will be set to the corresponding maximum demand for that trip class, \bar{q}_{rs}^k . Otherwise, the auxiliary demand will be set to zero.

In iteration 1, the current demands $q_{rs}^{n=1}$ are 0, so the inverse demand functions all return results of infinite time. Therefore all of the auxiliary demands are set to the maximum demand, \bar{q}_{rs}^k .

Table 3.4 Initializing auxiliary demands at maximum demands

		Z_{14}	Z_{24}	Z_{34}
Time on shortest path $c_m^{rs^{n=1}} = \min_{\forall j} \{c_j^{rs} (t_a^{n=1})\}$		10.00	7.00	9.00
$D_{rs}^{-1}(q_{rs}^{n=1})$	Trip Class $k=1$	∞	∞	∞
	Trip Class $k=2$	∞	∞	∞
Auxiliary Demand $v_{rs}^{n=1}$	Trip Class $k=1$	20.00	9.00	12.00
	Trip Class $k=2$	7.00	4.00	10.00

Initial auxiliary link volumes $y_a^{n=1}$ are obtained by loading the auxiliary demands on to the current shortest paths.

Table 3.5 Initializing auxiliary link volumes: loading shortest paths

	L_1	L_2	L_3	L_4	L_5
Auxiliary volume $y_a^{n=1}$	27.00	13.00	22.00	0.00	0.00

Step 3: Find the best moving step with which to adjust the current set of flows and demands

In general, the best moving step is calculated by minimizing Equation 2.21 indexed to the current iteration. However, at iteration 1, $\alpha = 1$.

Step 4: Updating link flows and travel demands

Update travel demands within each trip class k by linearly combining the current travel demands and the auxiliary travel demands using the value $\alpha = 1.0$.

$$q_{rs}^{n+1=2} = q_{rs}^{n=1} + 1.0 \cdot (v_{rs}^{n=1} - q_{rs}^{n=1}) \quad (3.11)$$

Table 3.6 Updating initial zero travel demand to auxiliary travel demand

		Z_{14}	Z_{24}	Z_{34}
Demand, $q_{rs}^{n+1=2}$	Trip Class $k=1$	20.00	9.00	12.00
	Trip Class $k=2$	7.00	4.00	10.00

Update link flows by linearly combining the current link volumes and the auxiliary link volumes using the value $\alpha = 1.0$.

$$x_a^{n+1=2} = x_a^{n=1} + 1.0 \cdot (y_a^{n=1} - x_a^{n=1}) \quad (3.12)$$

Table 3.7 Updating initial zero link flows to auxiliary link flows

	L_1	L_2	L_3	L_4	L_5
Link Volume, $x_a^{n+1=2}$	27.00	13.00	22.00	0.00	0.00

Since $\alpha = 1$ in iteration 1, the initial update consists of replacing the initial values of zero travel demand and zero link volumes with the auxiliary travel demand and link volumes computed in step 2.

Step 5: Convergence test

There will be no convergence at iteration 1. Set $n:=2$ and go to step 1, iteration 2.

3.2.2 Iteration 2

Step 1: Updating link travel times

The non-zero link volumes computed in iteration 1 produce large travel times on some used links.

Table 3.8 Updating link travel times in response to updated link flows

	L_1	L_2	L_3	L_4	L_5
Time, $t_a^{n=2} = t_a(x_a^{n=2})$	204.62	8.45	253.02	4.00	4.00

Step 2: Updating auxiliary travel demands and auxiliary link volumes

At the conclusion of the previous iteration, the travel demands were set to the values of auxiliary demands, which at this point are equal to the maximum demands, \bar{q}_{rs}^k . Consequently, the inverse of demand functions, $D_{rs}^k^{-1}(\bar{q}_{rs}^k)$, produce the lowest possible travel-time values. Given the current set of flows, some links are already congested. At this point, none of the travel times on the shortest paths are less than $D_{rs}^k^{-1}(\bar{q}_{rs}^k)$, so all of the corresponding auxiliary demands $v_{rs}^{n=2}$ are zero.

Table 3.9 Updating auxiliary travel demands in response to link travel times

		Z_{14}	Z_{24}	Z_{34}
Time on shortest path $c_m^{rs, n=2} = \min_{\forall j} \{c_j^{rs}(t_a^{n=2})\}$		12.45	8.45	12.45
$D_{rs}^{-1}(q_{rs}^{n=2})$	Trip Class 1	8.88	7.70	7.05
	Trip Class 2	6.77	8.15	6.77
Auxiliary Demand, $v_{rs}^{n=2}$	Trip Class 1	0.00	0.00	0.00
	Trip Class 2	0.00	0.00	0.00

These zero auxiliary demands are loaded on to the shortest paths to yield zero auxiliary link volumes $y_a^{n=2}$.

Table 3.10 Updating auxiliary link volumes: loading shortest paths

	L_1	L_2	L_3	L_4	L_5
Auxiliary volume $y_a^{n=2}$	0.00	0.00	0.00	0.00	0.00

Step 3: Find the best moving step with which to adjust the current set of flows and demands

Solve the following optimization problem with respect to α , yielding $\alpha=0.5256$.

$$\min z(\alpha) = \sum_a \int_0^{x_a^{n=2} + \alpha(y_a^{n=2} - x_a^{n=2})} t_a(w)dw - \sum_{r,s} \int_0^{q_{rs}^{n=2} + \alpha(v_{rs}^{n=2} - q_{rs}^{n=2})} D_{rs}^{-1}(w)dw \quad (3.13)$$

Step 4: Updating link flows and travel demands

Update travel demands by linearly combining the current travel demands and the auxiliary travel demands using the value $\alpha = 0.5256$.

$$q_{rs}^{n+1=3} = q_{rs}^{n=2} + 0.5256 \cdot (v_{rs}^{n=2} - q_{rs}^{n=2}) \quad (3.14)$$

Table 3.11 Updating travel demand, $\alpha = 0.5256$

		Z_{14}	Z_{24}	Z_{34}
Demand, $q_{rs}^{n+1=3}$	Trip Class 1	9.49	4.27	5.69
	Trip Class 2	3.32	1.90	4.74

Update link flows by linearly combining the current link volumes and the auxiliary link volumes using the value $\alpha = 0.5256$.

$$x_a^{n+1=3} = x_a^{n=2} + 0.5256 \cdot (y_a^{n=2} - x_a^{n=2}) \quad (3.15)$$

Table 3.12 Updating link volumes, $\alpha = 0.5256$

	L_1	L_2	L_3	L_4	L_5
Link Volume, $x_a^{n+1=3}$	12.81	6.17	10.44	0	0

Some links are still as yet unused because the associated free-flow travel times are larger than the congested travel times on competing routes.

Step 5: Convergence test

There will be no convergence at iteration 2. Set $n:=3$ and go to step 1, iteration 3.

3.2.3 Iteration 3

Step 1: Updating link travel times

The very high link travel times identified in iteration 2 are quickly being reduced as travel demands and link volumes are adjusted.

Table 3.13 Updating link travel times in response to updated link flows

	L_1	L_2	L_3	L_4	L_5
Time, $t_a^{n=3} = t_a(x_a^{n=3})$	19.86	7.07	21.36	4.00	4.00

Step 2: Updating auxiliary travel demands and auxiliary link volumes

As travel times on used paths are equalized, the travel times on the shortest paths are lower than $D_{rs}^{k-1}(q_{rs}^{n=3})$, giving maximum demand within each travel class, \bar{q}_{rs}^k , as the auxiliary demand.

Table 3.14 Updating auxiliary travel demands in response to link travel times

		Z_{14}	Z_{24}	Z_{34}
Time on shortest path $c_m^{rs, n=3} = \min_{\forall j} \{c_j^{rs}(t_a^{n=3})\}$		11.07	7.07	11.07
$D_{rs}^{-1}(q_{rs}^{n=3})$	Trip Class $k=1$	16.33	15.16	14.51
	Trip Class $k=2$	21.68	23.06	21.68
Auxiliary Demand, $v_{rs}^{n=3}$	Trip Class $k=1$	20.00	9.00	12.00
	Trip Class $k=2$	7.00	4.00	10.00

These auxiliary demands are loaded onto the shortest paths to yield auxiliary link volumes $y_a^{n=3}$.

Table 3.15 Updating auxiliary link volumes: loading shortest paths

	L_1	L_2	L_3	L_4	L_5
Auxiliary volume, $y_a^{n=3}$	0.00	62.00	0.00	27.00	22.00

Step 3: Find the best moving step with which to adjust the current set of flows and demands

Solve following optimization problem with respect to α , yielding $\alpha = 0.1647$.

$$\min z(\alpha) = \sum_a \int_0^{x_a^{n=3} + \alpha(y_a^{n=3} - x_a^{n=3})} t_a(w) dw - \sum_{r,s} \int_0^{q_{rs}^{n=3} + \alpha(v_{rs}^{n=3} - q_{rs}^{n=3})} D_{rs}^{-1}(w) dw \quad (3.16)$$

Step 4: Updating link flows and travel demands

Update travel demands by linearly combining the current travel demands and the auxiliary travel demands using the value $\alpha = 0.1647$.

$$q_{rs}^{n+1=4} = q_{rs}^{n=3} + 0.1647 \cdot (v_{rs}^{n=3} - q_{rs}^{n=3}) \quad (3.17)$$

Table 3.16 Updating travel demand, $\alpha = 0.1647$

		Z_{14}	Z_{24}	Z_{34}
Demand, $q_{rs}^{n+1=4}$	Trip Class $k=1$	11.22	5.05	6.73
	Trip Class $k=2$	3.92	2.24	5.60

Update link flows by linearly combining the current link volumes and the auxiliary link volumes using the value $\alpha = 0.1647$.

$$x_a^{n+1=4} = x_a^{n=3} + 0.1647 \cdot (y_a^{n=3} - x_a^{n=3}) \quad (3.18)$$

Table 3.17 Updating link volumes, $\alpha = 0.1647$

	L_1	L_2	L_3	L_4	L_5
Link Volume, $x_a^{n+1=4}$	10.70	15.36	8.72	4.45	3.62

Step 5: Convergence test

All five links are now accommodating flow. However, comparing the travel times for alternative paths, it is clear that the model has not yet converged. For example, the travel time on path L_4+L_2 is about twice (19.81 minutes) that of the travel time on link L_1 (10.70 minutes). Both paths serve zone-pair Z_{14} , and at user equilibrium should have equal travel times.

Table 3.18 summarizes the zone-to-zone travel demands and shortest path travel times associated with the first 30 iterations of the algorithm. Table 3.19 summarizes the corresponding link travel times and volumes.

3.3 VALIDATING EQUILIBRIUM CONDITIONS

In this small example, the algorithm solves for eight unknowns, three travel demands, and five link volumes by iteratively updating linear combinations of current and auxiliary variables. This secant method shows rather poor convergence after the first few iterations. Tables 3.18–3.19 show that the adjustment for travel demands and other unknowns is fairly rapid up to 4th iteration. After that, even for this example problem, values calculated in subsequent iterations tend to oscillate. The algorithm's convergence rate would not improve for a medium-sized real-world problem that might consist of several hundreds of traffic analysis zones (TAZs) and tens of thousands of network links. As a result, subsequent calculations, such as efforts to estimate the social cost of network damage, must be performed with caution.

One implication of this slow convergence rate is that the results produced may not completely conform to equilibrium conditions. The problem's two types of equilibrium conditions, equal travel times on competing routes and consistency between travel-demand zone-to-zone travel times, can be met only if the calculations fully converge.

Table 3.18 Travel demands and shortest path times for baseline example of variable-demand model: iterations 1–30

Iteration n	Demand, q_{rs}^n , Trip Class $k=1$			Demand, q_{rs} , Trip Class $k=2$			Shortest Path Travel Time, $c_m^{rs^n}$			α
	Z_{14}	Z_{24}	Z_{34}	Z_{14}	Z_{24}	Z_{34}	Z_{14}	Z_{24}	Z_{34}	
1	9.49	4.27	5.69	3.32	1.90	4.74	12.45	8.45	12.45	0.5256
2	11.22	5.05	6.73	3.93	2.24	5.61	11.07	7.07	11.07	0.1647
3	9.15	5.78	5.49	4.49	2.57	6.42	14.80	9.82	15.02	0.1845
4	9.68	5.94	5.81	4.62	2.64	6.60	13.69	9.51	14.08	0.0489
5	10.10	6.06	5.57	4.71	2.69	6.73	15.07	10.24	14.48	0.0404
6	10.33	6.13	5.72	4.60	2.72	6.81	15.04	10.15	14.64	0.0234
7	9.99	6.22	5.54	4.45	2.77	6.58	15.83	10.48	15.51	0.0329
8	10.18	6.28	5.66	4.50	2.79	6.65	15.10	10.39	14.69	0.0192
9	10.28	6.30	5.60	4.52	2.80	6.58	15.47	10.34	15.40	0.0101
10	10.41	6.34	5.53	4.56	2.82	6.50	15.48	10.55	15.15	0.0131
11	10.08	6.42	5.36	4.41	2.85	6.61	15.90	10.51	14.84	0.0313
12	10.22	6.46	5.45	4.45	2.87	6.65	15.19	10.43	14.95	0.0140
13	10.29	6.48	5.41	4.47	2.88	6.61	15.54	10.39	15.19	0.0070
14	10.39	6.50	5.35	4.50	2.89	6.54	15.48	10.53	15.30	0.0107
15	10.27	6.53	5.43	4.44	2.90	6.58	15.83	10.50	15.03	0.0114
16	10.09	6.57	5.33	4.49	2.92	6.46	15.56	10.47	15.18	0.0174
17	10.19	6.60	5.40	4.51	2.93	6.50	15.42	10.42	15.03	0.0094
18	10.22	6.61	5.42	4.52	2.94	6.51	15.53	10.40	15.04	0.0035
19	10.12	6.63	5.37	4.48	2.95	6.54	15.64	10.54	15.23	0.0097
20	10.20	6.65	5.42	4.50	2.96	6.57	15.43	10.59	15.05	0.0084
30	10.23	6.71	5.33	4.50	3.03	6.57	15.62	10.64	15.18	0.0066

Table 3.19 Link volumes and link travel times for the numerical example of a variable-demand model: iterations 1–30

Iteration n	Link Travel Time $t_a^n = t_a(x_a^n)$					Link Volume x_a^n				
	L_1	L_2	L_3	L_4	L_5	L_1	L_2	L_3	L_4	L_5
1	204.62	8.45	253.02	4.00	4.00	12.81	6.17	10.44	0.00	0.00
2	19.86	7.07	21.36	4.00	4.00	10.70	15.36	8.72	4.45	3.62
3	14.80	9.82	15.02	6.89	5.28	10.02	14.92	8.96	3.63	2.95
4	13.69	9.51	15.70	5.28	4.56	10.85	15.91	8.52	3.45	3.89
5	15.07	10.24	14.48	5.05	5.69	11.50	15.79	8.58	3.31	3.73
6	16.41	10.15	14.64	4.89	5.43	11.23	16.19	8.89	3.70	3.64
7	15.83	10.48	15.51	5.39	5.30	10.86	16.09	8.60	3.58	3.52
8	15.10	10.39	14.69	5.21	5.14	11.17	16.03	8.86	3.51	3.45
9	15.70	10.34	15.41	5.12	5.05	11.06	16.27	8.77	3.75	3.42
10	15.48	10.55	15.15	5.46	5.01	11.27	16.23	8.65	3.70	3.37
11	15.90	10.51	14.84	5.38	4.96	10.91	16.13	8.69	3.58	3.27
12	15.19	10.43	14.95	5.22	4.85	11.14	16.08	8.88	3.53	3.22
13	15.64	10.39	15.48	5.15	4.80	11.06	16.25	8.82	3.70	3.20
14	15.48	10.53	15.30	5.38	4.78	11.23	16.22	8.72	3.66	3.17
15	15.83	10.50	15.03	5.32	4.74	11.10	16.18	8.88	3.61	3.13
16	15.56	10.47	15.47	5.26	4.71	11.03	16.12	8.72	3.55	3.08
17	15.42	10.42	15.03	5.18	4.66	11.18	16.09	8.85	3.52	3.05
18	15.72	10.40	15.38	5.14	4.64	11.14	16.26	8.81	3.60	3.11
19	15.64	10.54	15.29	5.25	4.70	11.03	16.32	8.73	3.57	3.18
20	15.43	10.59	15.05	5.20	4.76	11.17	16.29	8.84	3.54	3.15
30	15.62	10.64	15.18	5.14	4.71	11.24	16.35	8.78	3.50	3.11

In this example problem, travel between two of the zone pairs may take place on competing routes. The paths L_1 , and L_4+L_2 are used to satisfy travel demand D_{14} . The paths L_3 , and L_5+L_2 are used to satisfy travel demand D_{34} . To compare the travel times on these competing routes, results from the 30th iteration row in Table 3.19 are displayed in Figure 3.1. Travel times on competing paths are compared and summarized in Table 3.20. After 30 iterations, travel times on competing paths differ by about only 1%. Equilibrium conditions on these could be more closely satisfied with further iterations of the algorithm.

Consistency between travel demands and zone-to-zone travel times is verified by comparing travel demands calculated by the model to the travel demands given by the various demand functions for the zone-to-zone travel times calculated by the model. Table 3.21 summarizes the comparison.

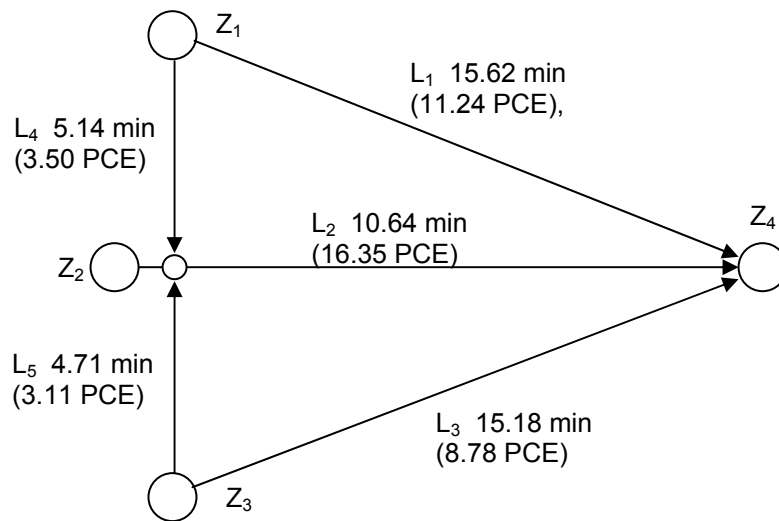


Fig. 3.2 Link travel times and volumes (passenger car equivalents) after 30 iterations

Table 3.20 Comparison of travel times on competing paths

Zone Pair	One-link Path		Two-link Path		B / A
	Travel Time (A)	Links	Travel Time (B)	Links	
D_{14}	15.62 min	L_1	15.78 min	L_4+L_2	1.010
D_{34}	15.18 min	L_3	15.30 min	L_5+L_2	1.008

Table 3.21 Comparison of travel demands, VDM and travel-demand function values

	VDM Travel Time (minutes) (A)	VDM Travel Demand (PCE) (B)	Travel-Demand Function Evaluated at VDM Travel Time (PCE) (C)	B / C ¹
D_{14}^1	15.62	10.23	10.19	1.004
D_{24}^1	10.64	6.71	6.71	1.001
D_{34}^1	15.18	5.33	5.33	1.000
D_{14}^2	15.62	4.50	4.50	1.001
D_{24}^2	10.64	3.03	3.53	0.857
D_{34}^2	15.18	6.57	6.57	1.000

Note: 1. Calculated to the fifth decimal and rounded to the fourth.

As Table 3.18 shows, the VDM's 30th iteration estimate for travel demand for trip class 1 between zones Z_1 and Z_4 is 10.23, and the shortest path travel time is 15.62 minutes. Applying this travel time to the demand function, $D_{14}^1 = 36.0 \cdot \exp(0.3 - 0.1 \cdot t_{14})$, yields 10.19 units of travel demand. If the VDM is completely converged, these two demand calculations should be identical.

As Table 3.21 shows, most of the estimated travel demands agree closely with the travel demands implied by travel times. The one exception is demand D_{24}^2 . Further, this difference persisted even after 200 iterations of the algorithm.

The secant method updates unknowns by a sequence of linear combinations in which all of the variables are adjusted by a single constant α in a direction that minimizes the value of the objective function. In practice, it seems that the objective function value improves rapidly in the first few iterations of the algorithm in response to adjustments dominated by the highest demand zone pairs. After this, once the impact of the largest travel demands have been accounted for, further adjustments that would achieve consistency between travel times for zone pairs

exhibiting low travel demand and these travel-demand values become very slow—so much so that convergence cannot be guaranteed. The result may be numerical oscillation.

A more sophisticated algorithm that involves updates incorporating more than one moving step size might be able to overcome this behavior, but this would greatly complicate the objective of ensuring feasible network flows at every step in the algorithm. This feasibility is an attractive aspect of the algorithm because the procedure can be stopped at any point with a solution that is physically meaningful even if all of the economic conditions that define equilibrium flows have not been fully met.

Alternatively, it may be that even this example problem includes an inherent infeasibility. There may be no set of flows that fully satisfy user-equilibrium conditions while at the same time providing travel demands fully consistent with the equilibrium cost of travel on use paths.

4 Applications to a Damaged Transportation Network

In the previous chapter, we focus on a simple network to study the convergence of the variable-demand model and the quality of its results. This chapter examines the behavior of the VDM results in response to damage to the transportation network, such as would occur in an earthquake. The same example network is considered when subjected to two damage scenarios. The social costs of forgone travel are calculated for each scenario.

4.1 SCENARIO 1 — SEVER LINK L_2

Severing link L_2 will necessarily cause considerable disruption of flows in this example. For Z_2 , L_2 is the only route that connects origin Z_2 to the destination, Z_4 . In the cases of Z_1 and Z_3 , severing L_2 eliminates only one of two alternative paths to Z_4 . These eliminated paths include links L_4 and L_5 , respectively (Fig. 4.1).

To model the impact of this severed link, the free-flow travel-time parameter in the corresponding BPR function is multiplied by an arbitrary large number (10^4), and the function's effective capacity parameter is divided by the same value. This makes travel on the link sufficiently expensive that it remains unused despite the presence of travel demands D_{24}^1 and D_{24}^2 .

Table 4.1 summarizes the travel-demand and travel-time values calculated for the first 30 iterations of the algorithm. The zero travel demand originating at zone Z_2 is noteworthy. This is a theoretically and computationally useful result because severing link L_2 has isolated Z_2 from the rest of the network. If travel demands were constant, as is the case in standard transportation planning applications, a zone isolated by damage to the network would result in an infeasible formulation with no solution. In this case, the absence of travel to or from an isolated zone is

handled endogenously, and predicted travel flows retain the user-equilibrium characteristics desired.

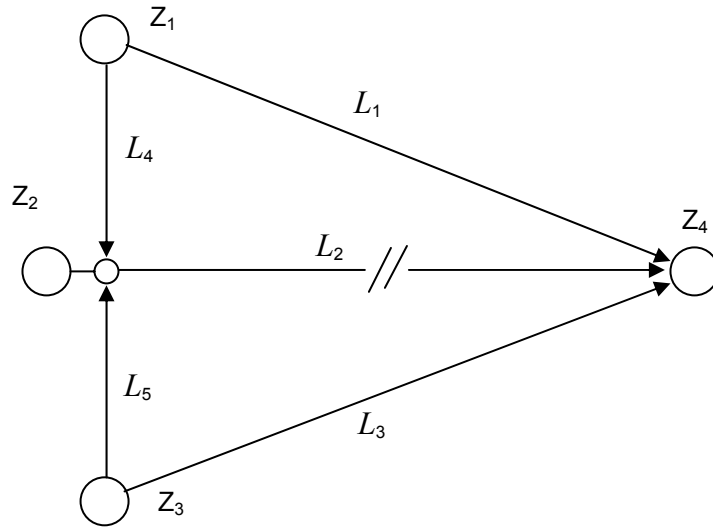


Fig. 4.1 Network configuration for scenario 1 — sever link L_2

Severing L_2 also affects the network level of service sufficiently to modify travel demands D_{14} and D_{34} . Table 4.2 compares the baseline travel times and travel demands from the previous section with the results for scenario 1. Overall, there is a system-wide reduction in travel times of more than 10%. Total travel time in the system increases by 14%.

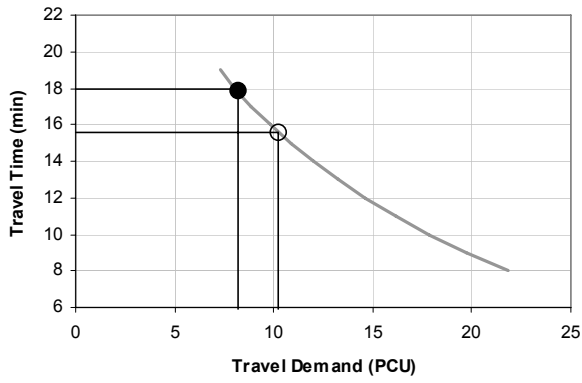
The travel-demand function coefficients for trip class 1 and trip class 2 are -0.1 and -0.05, respectively. This implies that demand for trips in class 2 is less elastic with respect to travel time changes, so the increase in travel times reduces trips in class 2 for those zone pairs for which flow remains feasible relatively less than in trip class 1, 12.8% versus 21.1%.

In Figure 4.2, each zone pair's baseline and scenario 1 travel demands travel times are plotted against the associated inverse demand curve. Convergence for scenario 1 appears to be complete.

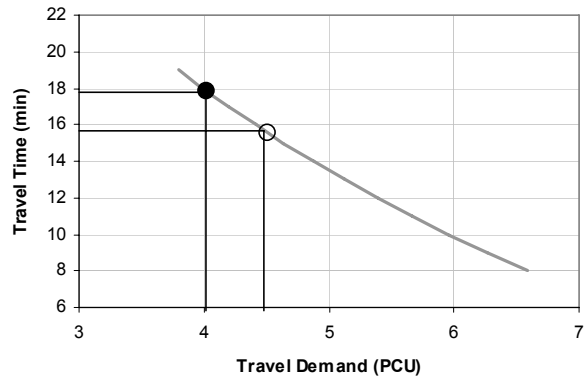
As Figure 2.3 depicts, the effect of eliminating network capacity can be divided into two parts. These are (1) the additional travel time experienced by travelers who continue to use the system and (2) value of forgone trips. The travel times for scenario 1 in Figures 4.2(e) and (f) are slightly greater than the inverse demand curves D_{34}^1 and D_{34}^2 imply, but overall these results conform closely to the conceptual diagram in Figure 2.3. As a result, for most of the zone pairs the calculation of the economic impacts associated with scenario 1 is straightforward.

Table 4.1 Travel demands and shortest path times for scenario 1: iterations 1–30

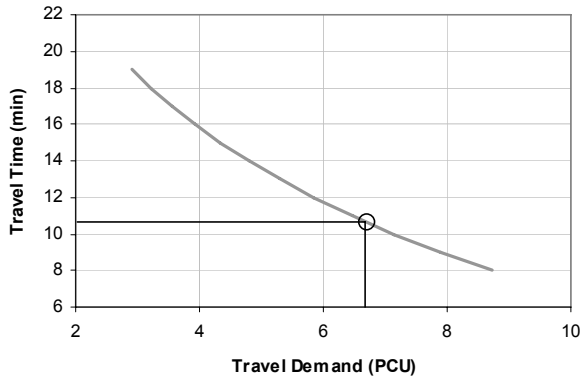
Iteration n	Demand, q_{rs}^n , Trip Class $k=1$			Demand, q_{rs} , Trip Class $k=2$			Shortest Path Travel Time, $c_m^{rs^n}$			α
	Z_{14}	Z_{24}	Z_{34}	Z_{14}	Z_{24}	Z_{34}	Z_{14}	Z_{24}	Z_{34}	
1	0.20	0.09	0.12	0.07	0.04	0.10	204.62	-	253.02	1.0000
2	19.80	-	11.88	6.93	-	9.90	10.00	-	9.00	1.0000
3	4.89	-	2.94	1.71	-	2.45	197.03	-	243.50	0.7528
4	9.32	-	5.59	3.26	-	4.66	10.70	-	9.88	0.2929
5	7.11	-	4.26	4.15	-	5.93	19.17	-	20.50	0.2371
6	7.96	-	3.98	4.34	-	5.53	15.88	-	20.23	0.0662
7	7.75	-	4.19	4.22	-	5.65	18.38	-	17.54	0.0264
8	8.22	-	4.04	4.06	-	5.44	17.53	-	18.79	0.0380
9	8.02	-	4.23	3.96	-	5.55	18.32	-	17.38	0.0242
10	8.35	-	4.11	4.05	-	5.67	17.55	-	18.51	0.0274
11	8.11	-	4.00	3.93	-	5.51	18.64	-	18.53	0.0279
12	8.30	-	4.13	3.98	-	5.58	17.71	-	17.51	0.0160
13	8.04	-	3.99	3.85	-	5.72	18.34	-	18.25	0.0322
14	8.28	-	3.91	3.92	-	5.61	17.32	-	18.29	0.0203
15	8.08	-	4.10	3.99	-	5.71	18.10	-	17.56	0.0237
16	8.27	-	4.04	4.04	-	5.62	17.78	-	18.67	0.0155
17	8.02	-	3.92	3.92	-	5.75	18.39	-	18.09	0.0294
18	8.26	-	4.08	3.98	-	5.64	17.45	-	18.12	0.0198
19	8.13	-	4.02	3.92	-	5.55	18.22	-	18.30	0.0155
20	8.27	-	4.11	3.95	-	5.60	17.72	-	17.73	0.0117
30	8.23	-	4.04	4.02	-	5.63	17.85	-	18.50	0.0103



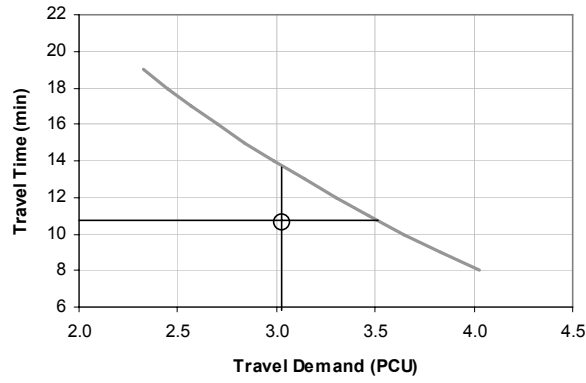
(a) D_{14}^1



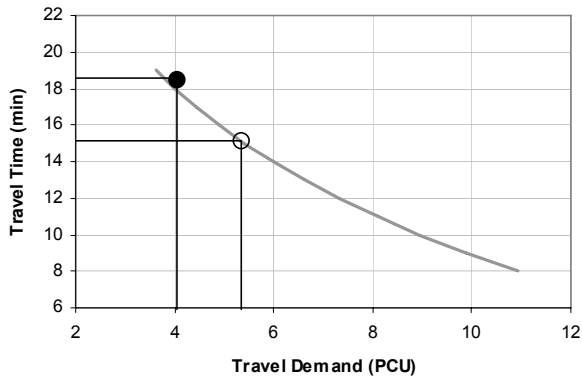
(b) D_{14}^2



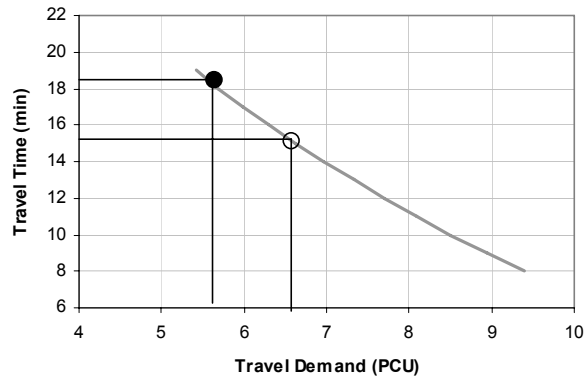
(c) D_{24}^1



(d) D_{24}^2



(e) D_{34}^1



(f) D_{34}^2

○ Baseline Trips and Travel Times

● Scenario 1 Trips and Travel Times

Fig. 4.2 Travel demands and travel times: baseline vs. scenario 1

$$D_{24}^2 = 5.58 \cdot \exp(0.002 - 0.05 \cdot t_{24}). \quad (4.1)$$

This step is a mere mathematical contrivance. In practice, travel-demand curves are empirically estimated from travel conditions, and are not subject to arbitrary adjustments. We make the adjustment here as an example of a first-order approximation.

Figure 4.3 shows this adjustment graphically. The area beneath this adjusted demand curve gives the value of forgone trips between the corresponding zone pair. Table 4.3 summarizes the costs of severing link L_2 . The value of trips forgone between zones Z_2 and Z_4 constitute a significant share of the total impact, in this case 66.8% of the total impact.

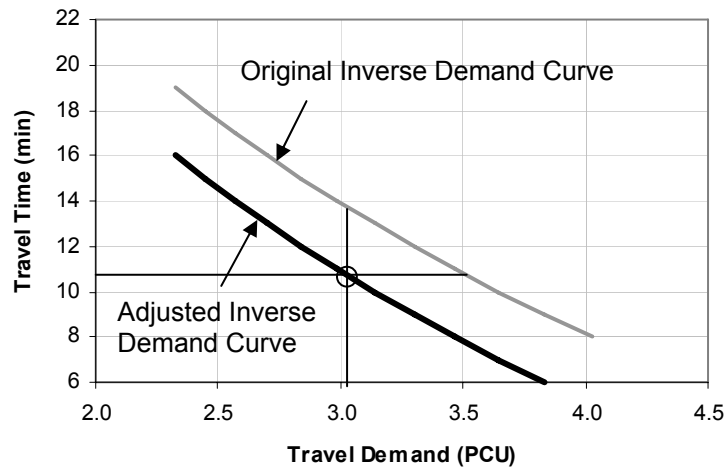


Fig. 4.3 Adjusting \bar{q}_{24}^2 to achieve a feasible solution describing baseline conditions

4.2 SCENARIO 2 — SEVER LINK L_4

Severing link L_4 eliminates one of the two alternative routes between zones Z_1 and Z_4 . This travel demand will be accommodated only on link L_1 , resulting in higher travel times and reduced travel demands D_{14}^1 and D_{14}^2 (Fig. 4.4). At the same time, severing this link L_4 will eliminate some of the travel on link L_2 because this alternative path from zone Z_1 and Z_4 is no longer available. This will reduce travel times for trips between zones Z_2 and Z_4 and between zones Z_3 and Z_4 , and increased travel demands $D_{24}^1, D_{24}^2, D_{34}^1$, and D_{34}^2 . Table 4.4 summarizes the travel-demand and travel-time values calculated for the first 30 iterations of the algorithm.

Table 4.3 Impacts associated with scenario 1 (passenger car equivalent minutes)

	Total Additional Travel Time Experienced by Those Continuing to Travel	Time Value of Trips Forgone Due to Travel Time Increases	Sum
D_{14}^1	18.35	2.02	20.37
D_{14}^2	8.96	0.52	9.49
D_{24}^1	0.00	65.68	65.68
D_{24}^2	0.00	65.22	65.22
D_{34}^1	13.41	1.63	15.04
D_{34}^2	18.69	1.40	20.09
Total	59.42	136.47	195.89

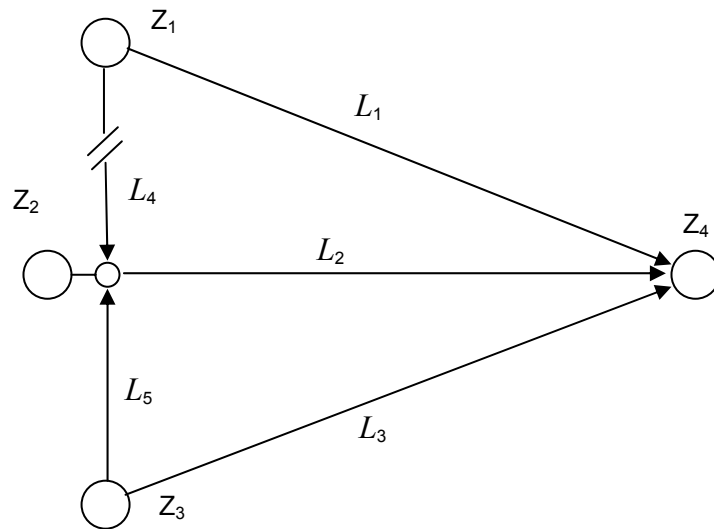


Fig. 4.4 Network configuration for scenario 2 — sever link L_4

The most notable result in scenario 2 is that eliminating some links in the network can cause improvements in the level of service experienced by some travelers. The changes are summarized in Table 4.5. Travel between zones Z_1 and Z_4 occurs with a 13.8% increase in travel time, leading to reductions of 20%, and 10% of travel demand in trip classes 1 and 2, respectively. In contrast, travel between zones Z_3 and Z_4 occurs with less competition for link L_2 , resulting in 5% reductions in travel times and attendant increases in travel demands.

Table 4.4 Travel demands and shortest path times for scenario 2: iterations 1–30

Iteration n	Demand, q_{rs}^n , Trip Class $k=1$			Demand, q_{rs} , Trip Class $k=2$			Shortest Path Travel Time, $c_m^{rs^n}$			α
	Z_{14}	Z_{24}	Z_{34}	Z_{14}	Z_{24}	Z_{34}	Z_{14}	Z_{24}	Z_{34}	
1	9.49	4.27	5.69	3.32	1.90	4.74	204.62	8.45	12.45	0.5256
2	7.48	5.27	7.02	4.10	2.34	5.85	19.86	7.07	11.07	0.2111
3	8.58	5.60	6.41	4.35	2.49	6.22	16.59	8.14	13.79	0.0878
4	7.69	5.95	5.74	3.90	2.65	6.61	20.26	8.17	14.16	0.1044
5	8.09	6.05	5.95	4.00	2.69	6.72	16.60	8.19	13.73	0.0330
6	8.35	6.11	6.07	4.06	2.72	6.79	17.84	8.51	13.88	0.0211
7	8.03	6.22	5.84	3.91	2.77	6.54	18.69	8.51	14.60	0.0376
8	8.34	6.30	6.00	3.99	2.80	6.63	17.45	8.50	13.81	0.0260
9	8.08	6.38	5.81	3.86	2.84	6.74	18.48	8.50	14.46	0.0318
10	8.34	6.44	5.95	3.93	2.86	6.81	17.45	8.65	14.01	0.0220
11	8.13	6.50	5.80	3.83	2.89	6.63	18.31	8.65	14.77	0.0254
12	8.34	6.55	5.91	3.89	2.91	6.69	17.50	8.64	14.21	0.0181
13	8.02	6.64	5.68	4.01	2.95	6.82	18.20	8.64	14.45	0.0386
14	8.22	6.68	5.79	4.06	2.97	6.88	17.68	8.83	13.99	0.0169
15	8.04	6.74	5.66	3.97	2.99	6.72	18.34	8.82	14.57	0.0225
16	8.23	6.77	5.76	4.02	3.01	6.77	17.62	8.81	14.09	0.0161
17	8.09	6.81	5.67	3.95	3.03	6.66	18.25	8.80	14.62	0.0167
18	8.24	6.84	5.74	3.99	3.04	6.70	17.71	8.80	14.28	0.0121
19	8.16	6.86	5.80	3.95	3.05	6.73	18.19	8.79	14.41	0.0096
20	7.87	6.93	5.59	4.06	3.08	6.85	17.88	8.90	14.48	0.0359
30	8.14	7.16	5.66	4.04	3.18	6.81	17.78	9.08	14.42	0.0075

Table 4.5 Changes in travel demands and travel times: baseline vs. scenario 2

	Travel Demand (Passenger Car Equivalents)			Travel Time (minutes)		
	Baseline	Scenario 2	$\Delta\%$	Baseline	Scenario 2	$\Delta\%$
D_{14}^1	10.23	8.14	(-20.0%)	15.62	17.78	13.8%
D_{14}^2	4.50	4.04	(-10.2%)			
D_{24}^1	6.71	7.16	6.7%	10.64	9.08	(-14.7%)
D_{24}^2	3.03	3.18	4.9%			
D_{34}^1	5.33	5.66	6.2%	15.18	14.42	(-5.0%)
D_{34}^2	6.57	6.81	3.7%			

Increases in travel demand as a result of isolated improvements in travel times is logical in a strict economic sense. If the variable-demand model proceeds as intended, improvements in equilibrium travel times will produce increases in travel demand. In the solution algorithm, auxiliary travel demand is either 0, or maximum demand, \bar{q}_{rs} , the demand for travel implied by zero travel time. However, these demand shifts are unlikely to be realized if the event eliminating links in the transportation network is an earthquake.

Most transportation planning applications of user-equilibrium models include the implicit assumption that travelers have perfect information concerning the level of service available on competing routes as well as the choices made by other travelers. This is reasonable in a long-run, steady-state context in which economic agents have an opportunity to inform themselves, possibly through trial and error, and make self-serving adjustments. Highway networks have been gradually improved by adding more capacity over several decades. Drivers have sufficient time to adjust and learn to make use of changes in network configurations.

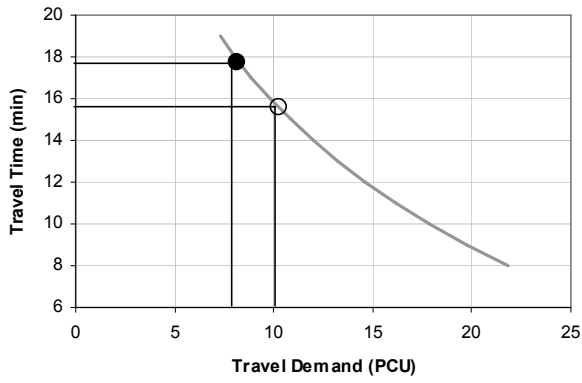
However, following an event such as a major earthquake, travelers likely would not make such long-term upward adjustments in travel demand in response to localized improvements in the level of service. In the interests of conservatism, we assume no level-of-service driven increases in travel demand, though decreases are still possible. Since their trip rate is not changed, the effective travel time does not change either.

Table 4.6 summarizes the calculations for scenario 2. After link L_4 is severed, travel demand between zones Z_2 and Z_3 , is held constant relative to the baseline, rather than being increased to a level consistent with the travel-demand function. The total impact of 29.0 PCE minutes is much less than that the impact in scenario 1 because no zones have been isolated from the network as a result of severing L_4 .

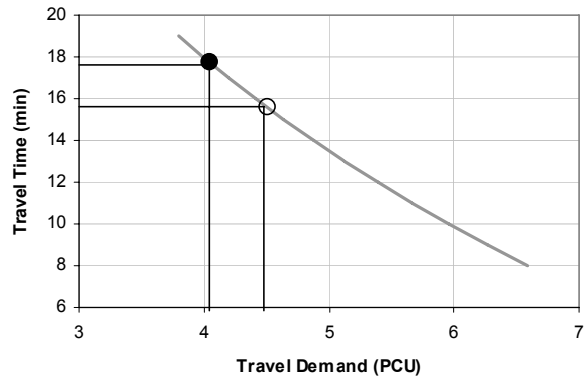
The plots in Figure 4.5 illustrate the baseline and scenario 2 travel demands and times for each trip class and zone pair. The plots of D_{24}^1 and D_{24}^2 show that the results for scenario 2 have the same feasibility problem that occurs in the baseline with respect to inverse demand function D_{24}^2 . The baseline inputs appear to be slightly infeasible, and thus computed travel demands do not conform to the given demand curve. In scenario 2, the same problem arises for all trips from zone Z_2 . This is less of a concern in this case because severing link L_4 increases demand for travel from zone Z_2 by diminishing competing demand accommodated on link L_4 , which remains unrealistic in the short term. As a result, these trips are not included in the calculation of impacts.

Table 4.6 Impacts associated with scenario 2 (passenger car equivalent minutes)

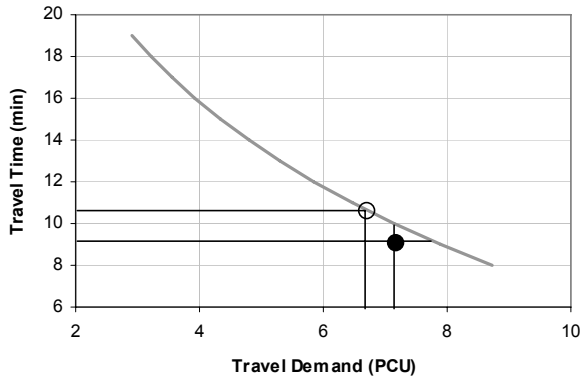
	Total Additional Travel Time Experienced by Those Continuing to Travel	Time Value of Trips Forgone Due to Travel-Time Increases	Sum
D_{14}^1	17.58	2.22	19.80
D_{14}^2	8.72	0.48	9.20
D_{24}^1	0.00	0.00	0.00
D_{24}^2	0.00	0.00	0.00
D_{34}^1	0.00	0.00	0.00
D_{34}^2	0.00	0.00	0.00
Total	26.30	2.70	29.00



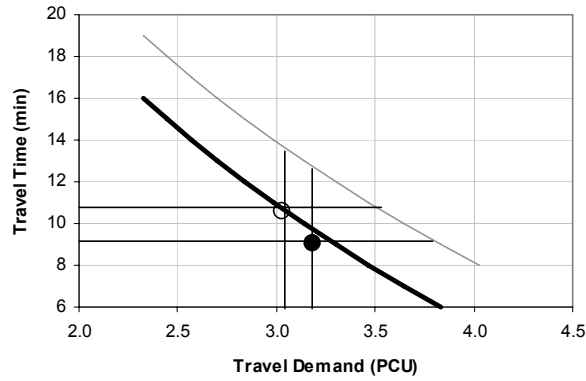
(a) D_{14}^1 ⁻¹



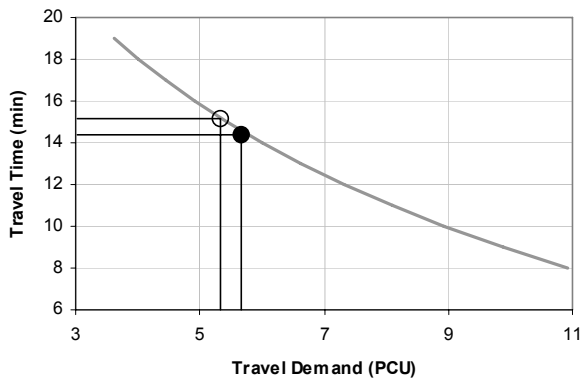
(b) D_{14}^2 ⁻¹



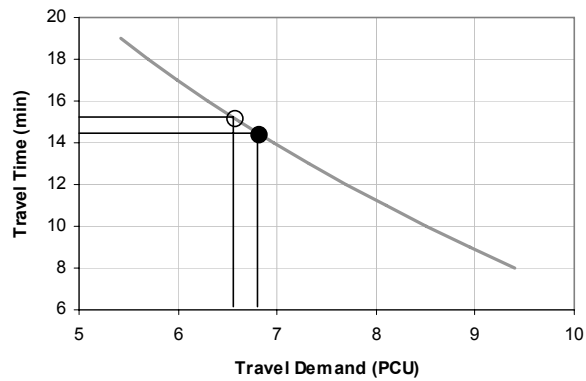
(c) D_{24}^1 ⁻¹



(d) D_{24}^2 ⁻¹



11(e) D_{34}^1 ⁻¹



11(f) D_{34}^2 ⁻¹

○ Baseline Trips and Travel Times

● Scenario 2 Trips and Travel Times

Fig. 4.5 Travel demands and travel times: baseline vs. scenario 2

As before, it is possible to shift the demand curve to match the baseline travel conditions. It is also possible to select a function that replicates the flows computed for scenario 2. In scenario 2, Equations 3.9 and 4.2 are replaced by

$$D_{24}^2 = 5.58 \cdot \exp(-0.2802 - 0.03106 \cdot t_{24}). \quad (4.2)$$

See Figure 4.6.

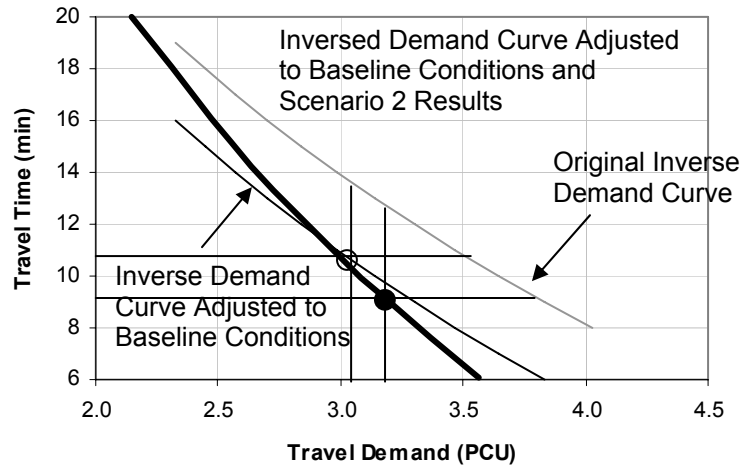


Fig. 4.6 Adjusting D_{24}^2 to achieve a feasible solution describing baseline conditions and scenario 2 results

4.3 CALCULATING THE TRANSPORTATION IMPACTS OF AN EARTH-QUAKE GIVEN VARIABLE DEMAND

Network changes, such as described in scenarios 1 and 2, are the sort of capacity losses produced by earthquake damage. We summarize the various ways these outputs can be used to calculate transportation impacts, noting that the VDM is sometimes unable to produce fully feasible estimates of baseline and post-earthquake travel flows. For simplicity, we use following abbreviations:

d_1 : Baseline trips

d_2 : Post-earthquake trips

t_1 : Baseline travel times

t_2 : Post-earthquake travel time

D : Travel-demand function

C_1 : Additional travel time accruing to travelers remaining on the network

C_2 : Value of trips forgone

4.3.1 Case 1: $d_1 = D(t_1)$, $d_2 = D(t_2)$, $d_1 > d_2$, and $t_1 < t_2$

The earthquake reduces demand for access by reducing capacity and increasing travel times. When a zone is isolated from the network, $d_2 = 0$, and $t_2 = \infty$. In this case the earthquake transportation cost calculations are as follows:

$$C_1 = d_2 \cdot (t_2 - t_1) \quad (4.3)$$

$$C_2 = \int_{t_1}^{t_2} D(w) dw - C_1 \quad (4.4)$$

4.3.2 Case 2: $d_1 = D(t_1)$, $d_2 = D(t_2)$, $d_1 < d_2$, and $t_1 > t_2$

The earthquake reduces demand for access by reducing capacity and increasing travel times, but this reduces competition for access to some links, producing local improvements in travel conditions. Rather than predict resulting increases in casual travel demand during an emergency, set $d_1 = d_2$, and $t_1 = t_2$, setting transportation cost impacts to zero.

4.3.3 Case 3: $d_1 \neq D(t_1)$

The baseline VDM solution is inconsistent with the given input demand function. The model's inputs are infeasible. Achieve feasibility by shifting the demand curve to set $d_1 = D(t_1)$, replicating Case 1 or 2.

4.3.4 Case 4: $d_2 \neq D(t_2)$

The post-earthquake VDM solution is inconsistent with the given input demand function. Achieve feasibility by shifting the demand curve to set $d_1 = D(t_1)$ and $d_2 = D(t_2)$.

5 Applying Variable-Demand Model to a Realistic Earthquake Impact Calculation

In this chapter, the VDM is applied to model the transportation and travel impacts of an intense earthquake scenario for the San Francisco Bay Area that includes significant damage to both the transportation network and the urban activity system. This example focuses on household travel demand for the sake of illustration, but corresponding procedures are available for freight flows.

Travel-demand data for freight and passenger demand are typically collected differently by Metropolitan Planning Organizations, and at different intervals. Freight demands are generally less well understood, but can be treated. For example, some urban freight flows are regional or national transshipments that would otherwise be directed to other locations following an earthquake. A key advance in freight modeling is the capacity to estimate the intensity of the freight demand based on knowledge of the urban activity system, rather than by more conventional survey methods (Gordon and Pan 2001).

Changes in freight travel demand can also be modeled in the variable-demand framework presented here if the initial freight origin-destination data are available (Kiremidjian et al. 2006). The Metropolitan Transportation Commission (MTC) does make a set of Bay Area freight origin-destination data available for professional and academic use, but we restrict our analysis to household travel demand for the sake of brevity. However, these procedures extend directly to the freight case, and any full cost analysis of transportation impacts resulting from earthquake damage would normally include freight as well as passenger demand for travel.

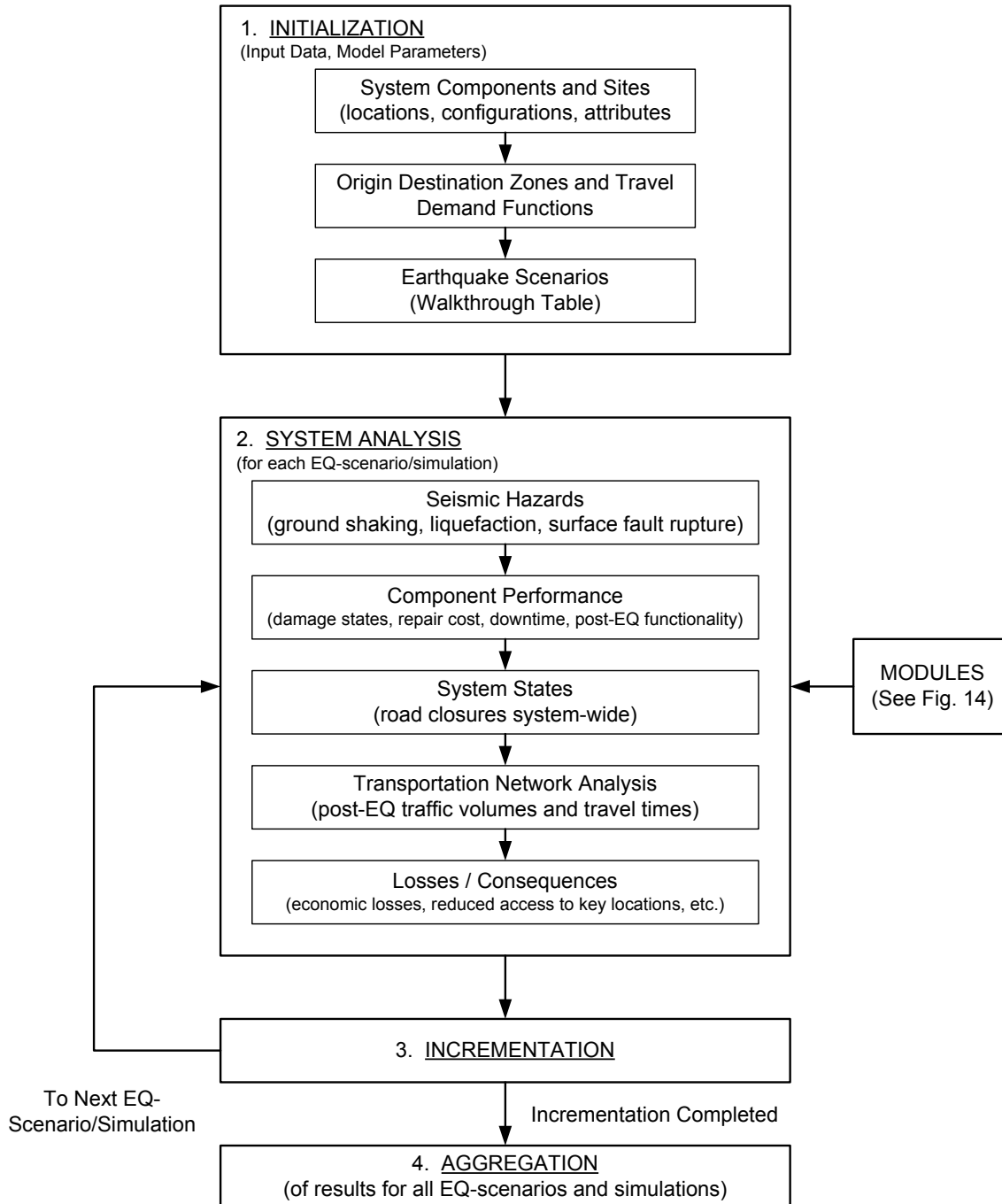
5.1 OVERVIEW OF REDARS (RISKS FROM EARTHQUAKE DAMAGE TO ROADWAY SYSTEMS)

REDARS, a software package supplied by the Federal Highway Administration (FHWA), is an advanced seismic risk analysis (SRA) tool that enables users to better plan for and respond to earthquake emergencies. The REDARS methodology's risk-based framework uses models for seismology and geology, engineering (structural, geotechnical, and transportation), repair and reconstruction, system analysis, and economics to estimate system-wide direct losses and indirect losses due to reduced traffic flows and increased travel times caused by earthquake damage to the highway system. The results from this methodology also show how this damage can affect access to facilities critical to emergency response and recovery. REDARS was developed by FHWA and the Multi-Disciplinary Earthquake Engineering Research Center (MCEER) as a future public-domain software package, and is the most advanced and developed SRA methodology currently available. REDARS 2.0 incorporates a version of the variable-demand model operationalized in the PEER Highway Demonstration Project.

5.1.1 Features of REDARS Seismic Risk Analysis

The REDARS SRA methodology (Werner et al. 2000, 2006) is shown in Figure 5.1. It consists of input data and analysis setup (step 1), seismic analysis of the highway system for multiple scenario earthquakes and simulations (steps 2 and 3), and aggregation of the results from each analysis (step 4). In this, a simulation is defined as a complete set of system SRA results for one set of uncertain input and model parameters. The numerical values of these parameters for one simulation may differ from those of other simulations because of random and systematic uncertainties.

The SRA methodology uses a walk-through process (Taylor et al. 2001) that considers earthquake occurrences over a specified walk-through duration, which may be many years. For each year of the walk-through, random samplings of a regional earthquake model are used to establish the number of earthquakes, i.e., zero, one, or more events, occurring during that year, along with each earthquake's magnitude and location.

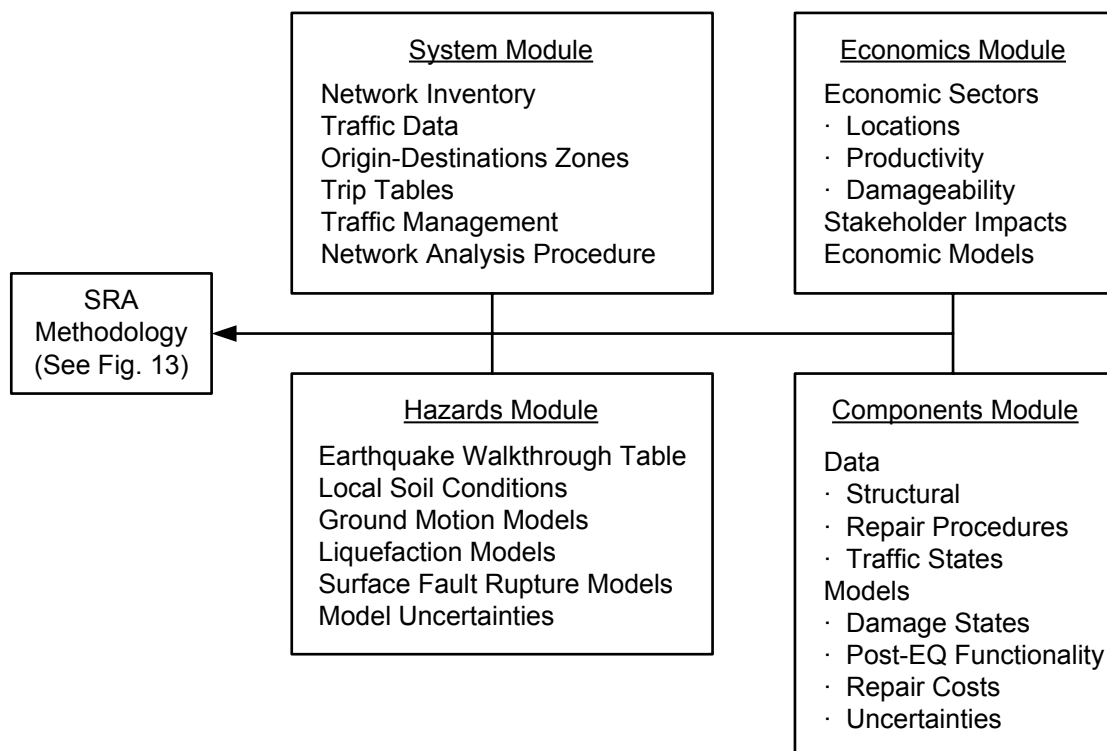


Source: Werner et al. (2000) *A Risk-Based Methodology for Assessing the Seismic Performance of Highway Systems*, MCEER-00-0014

Fig. 5.1 REDARS methodology for seismic risk analysis of highway systems

These results are stored in a walk-through table that contains a year-by-year tabulation of these earthquake occurrences.

The heart of the methodology is a series of modules that contain the input data and analytical models needed to characterize the highway system, the seismic hazards, the fragility of the components within the system, and the economic losses due to earthquake-induced damage and traffic disruption (Fig. 5.2). This modular structure facilitates the inclusion of new improvements to REDARS' hazards, component, and network models, as they are developed from future research.



Source: Werner et al. (2000) *A Risk-Based Methodology for Assessing the Seismic Performance of Highway Systems*, MCEER-00-0014

Fig. 5.2 REDARS SRA modules

The SRA methodology is a synthesis of models developed by earth scientists, geotechnical and structural earthquake engineers, transportation engineers and transportation planners, and economists. As a result, the methodology can develop multiple types/forms of results from deterministic or probabilistic SRA to meet the needs of a wide range of possible future users.

5.1.2 REDARS Applications

REDARS was successfully applied to the Memphis, Tennessee, highway network, a location that is vulnerable to a repeat of the 1812 New Madrid zone earthquakes. The success of the Memphis study led to its application to the significantly more challenging California environment, where the earthquake sources are more pervasive, the highway network more extensive, and the economic consequences more profound. This California project was aimed at transferring technical expertise from the developer community within FHWA and MCEER to the California Department of Transportation (Caltrans) through a guided and carefully reviewed application of the REDARS methodology to a limited portion of the Caltrans highway network extending from Fairfield to Oakland.

5.2 BAY AREA TRANSPORTATION DATA

We apply the REDARS 2.0 import wizard to create the database used in this application. The import wizard is a tool that combines federal, state, and local data from public sources to generate transportation network data for the study area. The public data sources used to compile the network database consist of the following:

- the National Highway Planning Network (NHPN) from the Federal Highway Administration (FHWA),
- the FHWA Highway Performance Monitoring System (HPMS)
- FHWA National Bridge Inventory (NBI),
- the Bay Area transportation analysis zone map from the Metropolitan Transportation Commission (MTC), and
- the MTC 1998 Bay Area (passenger) trip table (Peak 4 hours).

Figure 5.3 shows the transportation network modeled for this exercise. The model includes 10,154 directional links; 3,288 nodes, including 1,136 zone centroids; 1,475 bridges; and eight tunnels. The data available in the NBI does not account for recent retrofits, and this will lead to pessimistic bridge damage predictions.

In a large network, travel-demand functions can be estimated empirically via an application of a gravity model that estimates a relationship between trip frequencies in the region

and travel time, and combines this function with estimates zone-specific coefficients that account for the urban activity system's impact on travel demand (Kiremidjian et al. 2006). Detailed empirical trip frequency data are difficult to accommodate in this framework, since the frequency of trip making does not decrease monotonically with respect to the travel times between zone pairs. Instead, the distribution of trip rates with respect to interzonal travel times peaks at a small positive value. For the origin-destination matrix for the San Francisco Bay Area, this peak is at travel times of about eight minutes.

For modeling purposes, this nonmonotonic relationship must be estimated with a best-fitting monotonic form (Fig. 5.4). This function is bounded above. For example, the maximum number of vehicle trips generated between a given origin-destination is bounded by the population size at the origin. These assumptions have the advantage of ensuring that the inverse travel-demand function can be defined, which provides analytical convenience.

5.3 HAYWARD FAULT SCENARIO EARTHQUAKE

The scenario earthquake is a moment magnitude 7.1 event along the Hayward fault with an epicenter at -122.0866 degrees/37.7266 degrees in decimal longitude and latitude. The black dot on Figure 5.5 represents the epicenter, and the dashed line is the Hayward fault line. From this intense earthquake, the REDARS 2.0 bridge model estimates 92 bridge collapses and 466 damaged bridges. In addition, 36 links would be subject to pavement failures due to liquefaction.

These estimates are generated by a version of REDARS that preceded the current degree of REDARS calibration achieved relative to the Northridge earthquake. The most recent revision to REDARS models predicts fewer bridge collapses and more extensive damage to roadway links due to liquefaction and surface fault rupture than this example provides. Predicted bridge damage and failures would be further reduced if retrofit efforts to date were accounted for in the NBI data.

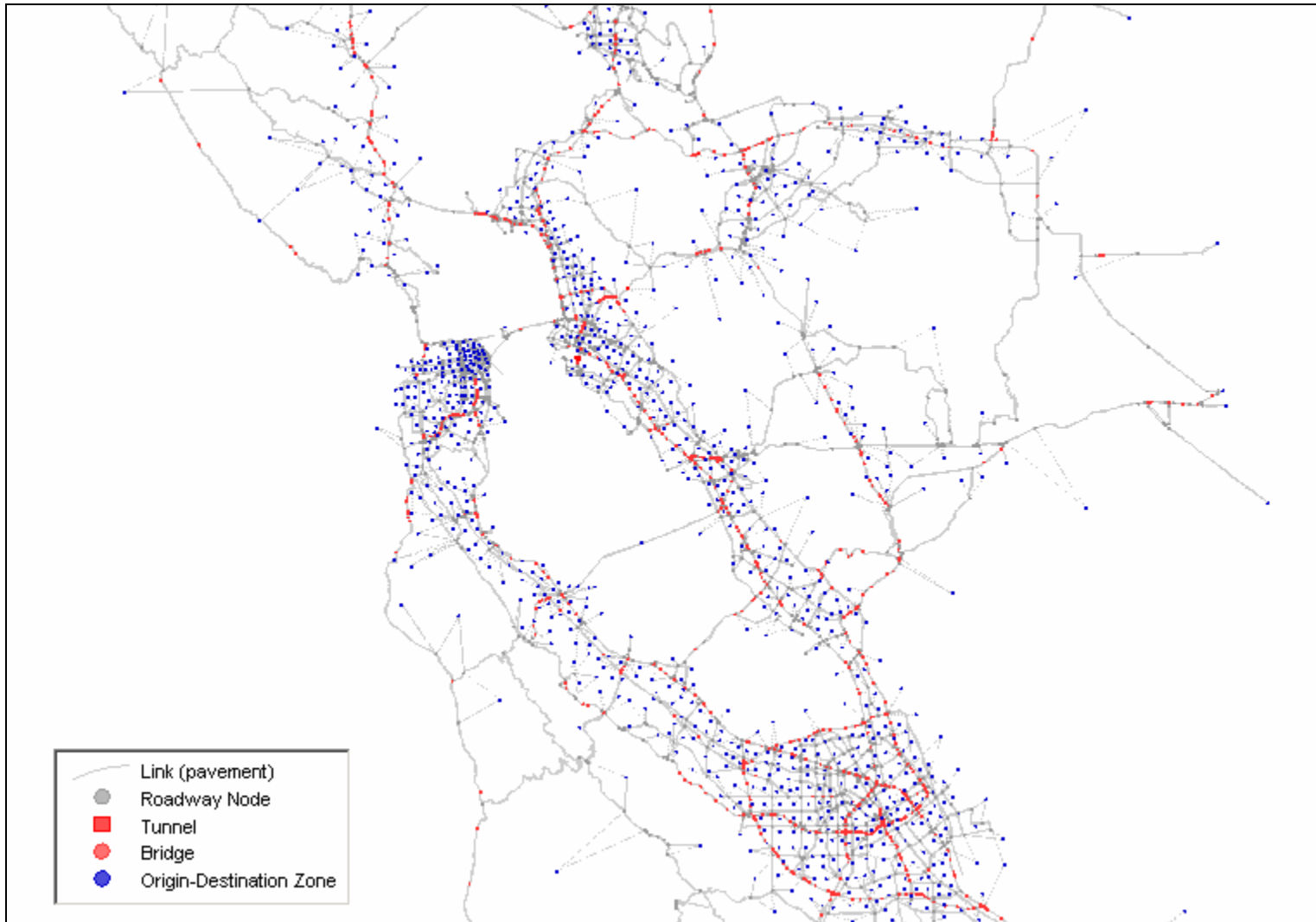
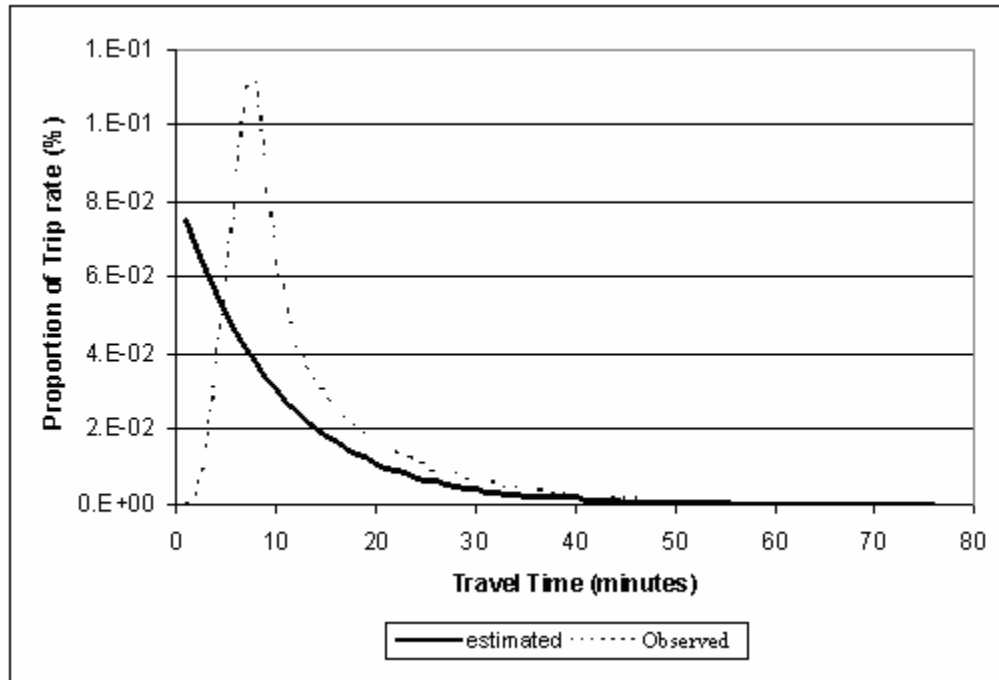


Fig. 5.3 San Francisco Bay Area roadway network characterized by REDARS 2.0 import wizard



Source: Kiremidjian et al. (2006) Pacific Earthquake Engineering Research Center Highway Demonstration Project Final Report 2006/02.

Fig. 5.4 Observed and estimated San Francisco Bay Area baseline interzonal trip rates as function of travel time

Figure 5.5 summarizes the damage states of the various highway components. This damage will gradually be repaired over time. REDARS 2.0 predicts staged network configurations at 7 days, 60 days, and 150 days after the earthquake using an empirical recovery model. The recovery model suggests that, with no special resource constraints, all collapsed and damaged bridges would be repaired or reconstructed within 231 days.

5.3.1 Modeling Network Performance and Economic Travel Choices

The VDM and the earthquake impact calculations are implemented in a set of computer codes, and incorporated into the REDARS 2.0 system. For a given earthquake scenario and network data, REDARS 2.0 sequentially analyzes ground motion, bridge / tunnel / roadway damage states, network configurations, and executes a VDM analysis of network level of service 7, 60, 150 days following the event.

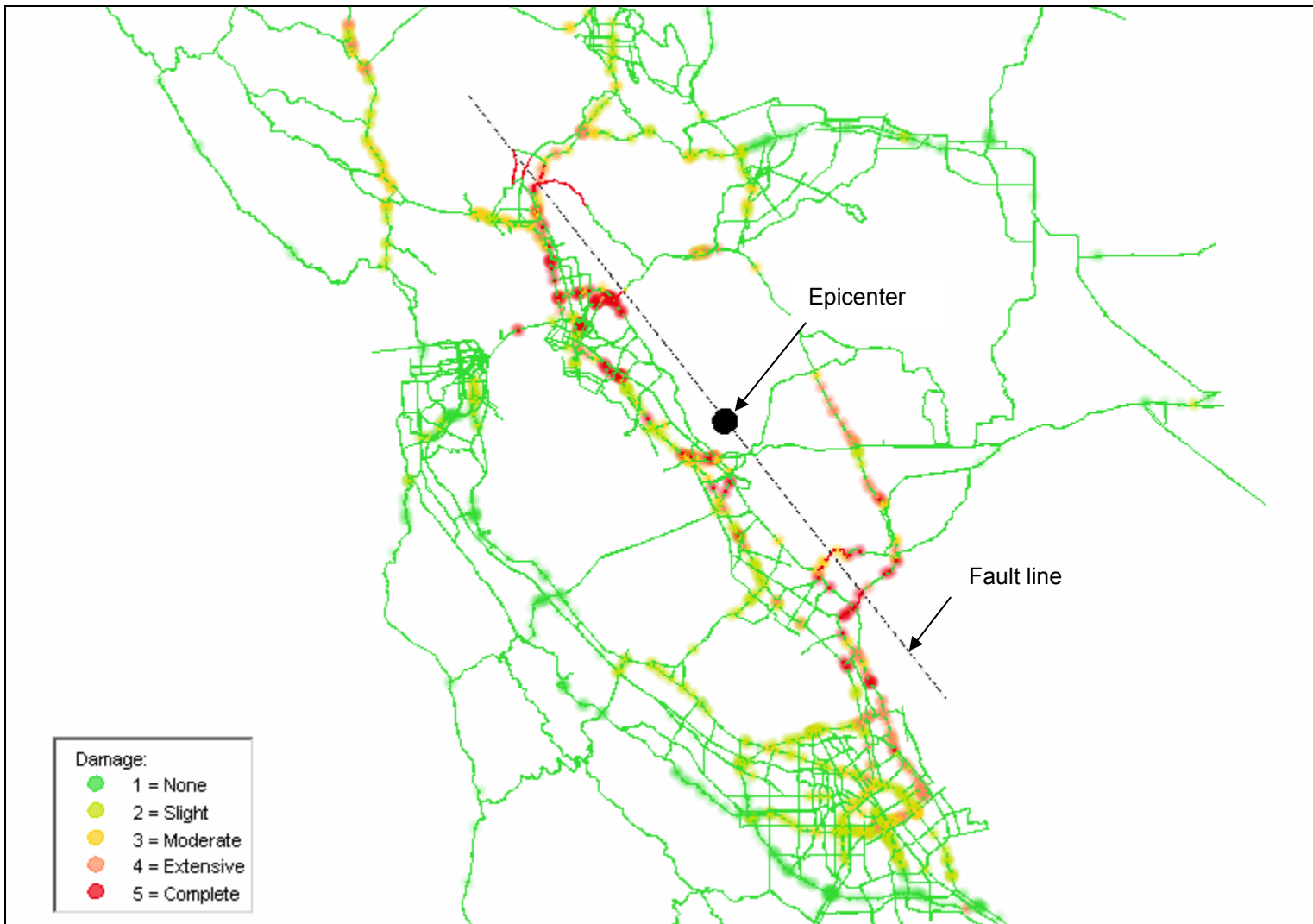


Fig. 5.5 Bridge and link damage states associated with Hayward fault scenario earthquake

After about four minutes of calculations using desktop computing resources, travel demands associated with only 20% of the origin-destination zone pairs have converged to values consistent with the associated set of empirically estimated travel-demand functions. However, the flows associated with these zone pairs account for 95% of the total trips in the system. The remaining 80% of the zone pairs account for only about 5% of the trips (Fig. 5.6).

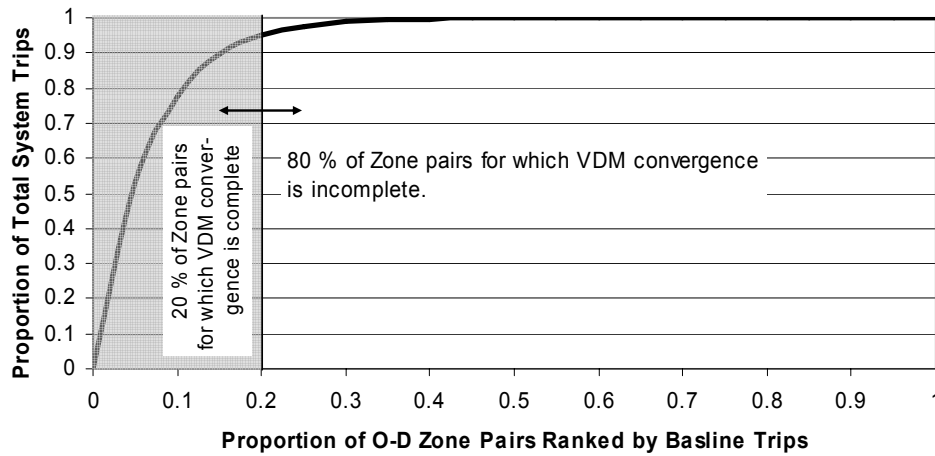


Fig. 5.6 VDM is most effective at accounting for elasticity of travel between zone pairs subject to intense travel demands

This result is both fortuitous and understandable. Given that the LeBlanc and Farhangian algorithm implemented to solve the VDM problem adjusts only a single search parameter α by solving an unconstrained optimization problem at each iteration, it is logical that the value of α identified will be strongly influenced by the largest interzonal flows. As result, convergence of the algorithm is relatively rapid with respect to the largest interzonal flows, at the cost of being very slow with respect to the smallest flows. Despite the fact that convergence with respect to the majority of interzonal flows is poor, the great majority of forgone trips can be still be identified and correctly evaluated using this approach; because the zone pairs for which convergence is poor, while numerous, account for a very small share of total baseline travel.

5.3.2 Economic Impacts: Accounting for Value of Forgone Trips

Table 5.1 summarizes network performance following the earthquake and during the course of recovery. Of 10,154 road links, 210 are severed as of the 7th day following the earthquake. This disruption causes a system-wide trip reduction of more than 30%. As repairs proceed and

capacity is restored, travel demand also recovers. By the 60th day, the trip making has reached about 94% of the pre-earthquake baseline, and by the 150th day 96% aggregate travel demand has reached 96% of the baseline. Due to the rapid recovery projected in this scenario, the value of forgone trips is quickly reduced from 14,600 PCE-hours on the 7th day to 3,300 PCE-hours by the 60th day, and 1,800 PCE-hours by the 150th day.

Table 5.1 Bay Area transportation impacts of the Hayward fault scenario earthquake

	7 Days After the Earthquake	60 Days After the Earthquake	150 Days After the Earthquake
Number of Severed Network Links	210	94	46
Total Trips (PCE)	847,535	1,169,352	1,193,284
Trip Reduction Relative to the Pre-earthquake Baseline (%)	31.5	5.5	3.6
Average Travel Time (Minutes)	43.37	42.74	42.17
Travel-Time Increase Relative to the Pre-earthquake Baseline (%)	8.30	6.73	5.29
Additional Travel Time Accruing to Remaining Trips (PCE-Hours)	38,236	49,218	40,230
Value of Forgone Trips (PCE-Hours)	14,605	3,339	1,808
Total Impact (PCE-Hours)	52,842	52,557	42,039
Daily Impact (\$Millions) ¹	3.80	3.78	3.03

Note: 1. Value of time: \$15/(person hour), average vehicle occupancy 1.2 persons/PCE, four peak hour conversion factor to daily impacts = 4.0.

In contrast, the additional travel time experienced by travelers remaining in the system stays high. This cost is calculated based on the number of post-earthquake trips and the difference between the baseline and post-earthquake travel times. Immediately following the earthquake, the substantial travel-time increases (8% on average, system-wide) relative to the baseline imposes large additional travel costs on the drivers still using the system, even though post-earthquake trip making is only 70% of the baseline level. In later periods, the 5.3%

difference in travel time and the resulting recovery in travel demands results in continued high incremental travel costs.

Assuming a value of time at \$15 per person-hour, and average vehicle occupancy of 1.2 persons per PCE, and a factor 4.0 for converting figures from the four-hour peak to a daily figure, the total travel impacts are \$3.80M per day, \$3.78M per day, and \$3.03M per day for at 7th, 60th, and 150th days following the earthquake, respectively. Exercising the recovery model in REDARS 2.0 produces an estimate that, given unlimited resources, system recovery could be achieved 231 days after the earthquake. The total transportation impacts that the scenario earthquake imposes on households is the area below the total impact curve in Figure 5.7. In this example scenario, the area is \$656.81M. These costs include increases only in transportation delays and the value of trips forgone due to reductions in the level of service. This total does not include the cost of repairs to transportation structures, nor the cost of freight flows forgone.

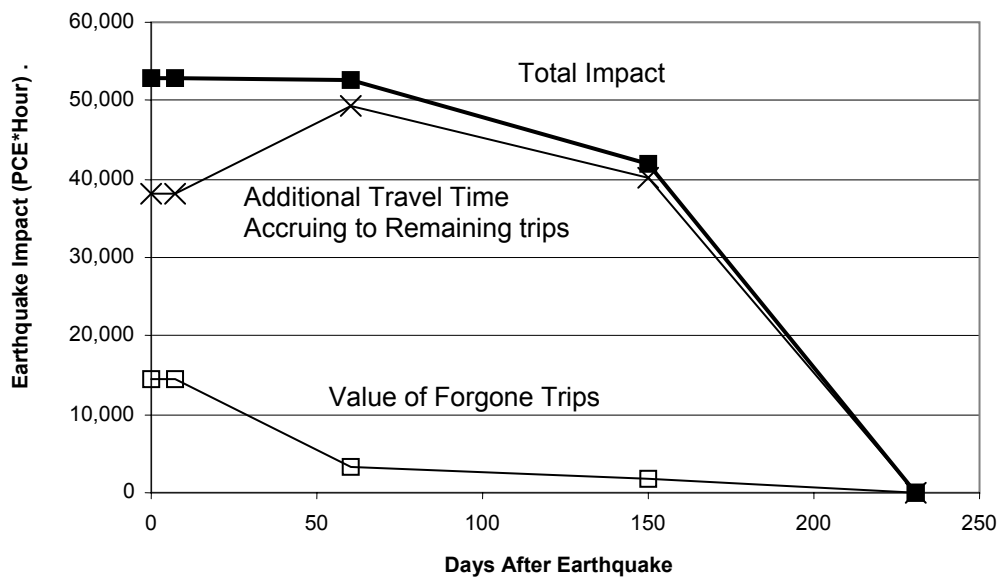


Fig. 5.7 Total household transportation impacts associated with Hayward fault scenario earthquake

6 Summary and Recommendations for Future Research

The highway system is one of the most important lifeline systems subject to natural and man-made hazards. The overarching objective of seismic risk research relating to road networks is to ensure a high level of reliability for continued operation of the system following an earthquake. The transportation system, in particular, is critical to the execution of emergency response tasks in addition to supporting the movement of people and goods crucial to local economies.

In our work to date on seismic risk analysis of highways, we have developed models for assessing the total economic loss due to transportation network disruption caused by given earthquake scenario. We have focused on travel time as the network performance measure, and converted time to its monetary value. Our work has allowed us to incrementally and substantially improve how standard transportation planning and modeling tools are applied to networks subject to earthquakes, first by modifying network flow models to account for how reduction in network level of service suppress demand for transportation services, and now by estimating the economic value of trips forgone when demand for travel is reduced. Further, we have met these objectives by focusing exclusively on the transportation network: We have not had to broaden our attention to include a model of the urban economy. This achievement is auspicious because travel is a derived demand and standard approaches do not separate models of travel demand from the economy's activity system.

6.1 PERFORMANCE OF THE ALGORITHM

The variable-demand model is a strong candidate for replacing standard implementation of user-equilibrium models in seismic risk analysis. This study investigates the efficacy of relaxing constant demand assumptions via a detailed implementation and application to estimate changes in travel times and travel demands in contrived and realistic applications. The mathematical

formulation is promising, but the solution algorithm is somewhat slow to converge, even in some simple examples, and the numerical solution can routinely oscillate. More importantly, the algorithm has difficulty identifying a fully feasible solution, and sometimes predicts flows that are inconsistent with the travel-demand functions specified for zone pairs subject to low travel demands.

Fortunately, the algorithm's tendency to minimize the Beckmann et al. (Eq. 2.8) by exploiting adjustments in the largest interzonal travel demands results in fully feasible mathematical results for the great majority of trips. Link flows computed at every iteration of the algorithm remain feasible for the nonlinear programming problem given by Equations 2.8–2.13, but the travel demands for many or even most zone pairs subject to low travel requirements remain numerically inconsistent with the inverse travel-demand functions that appear in the program's objective function. The version of the algorithm implemented here in detail to solve the variable-demand model is a modest improvement in the algorithm implemented by Kiremidjian et al. (2006). Further incremental improvements in the algorithm are feasible and desirable, and further investigation will yield them. However, the procedure is currently robust enough to deliver meaningful results in a large-scale application.

6.2 DEMAND SHIFTS VERSUS VARIABLE DEMAND FOR TRANSPORTATION

Our focus on the transportation system includes minimal attention to the urban activity system that generates the trips served by the transportation network. Large-scale land use / transportation models are data intensive, but useful models exist (An et al. 2004; Gordon et al. 2002). Extending this research to include impacts on the activity system is a logical step because earthquakes damage buildings in addition to transportation structures. This suppresses economic activity, and diminishes the demand for transportation. This sort of demand impact is distinct from the impacts accounted for by the VDM, which focuses on movement along a transportation demand curve following an earthquake-induced reduction in transportation supply. This is an important effect, but only part of the story.

A major earthquake will also produce attendant shifts in the transportation demand curve, leading to more trips forgone. Figure 6.1 describes this effect graphically. Figure 6.1(b) shows a simultaneous shift in demand and supply that holds equilibrium travel times constant. In this

special case, economic losses accrue only to the travelers who no longer take trips, but the total potential cost of travel forgone is substantially increased.

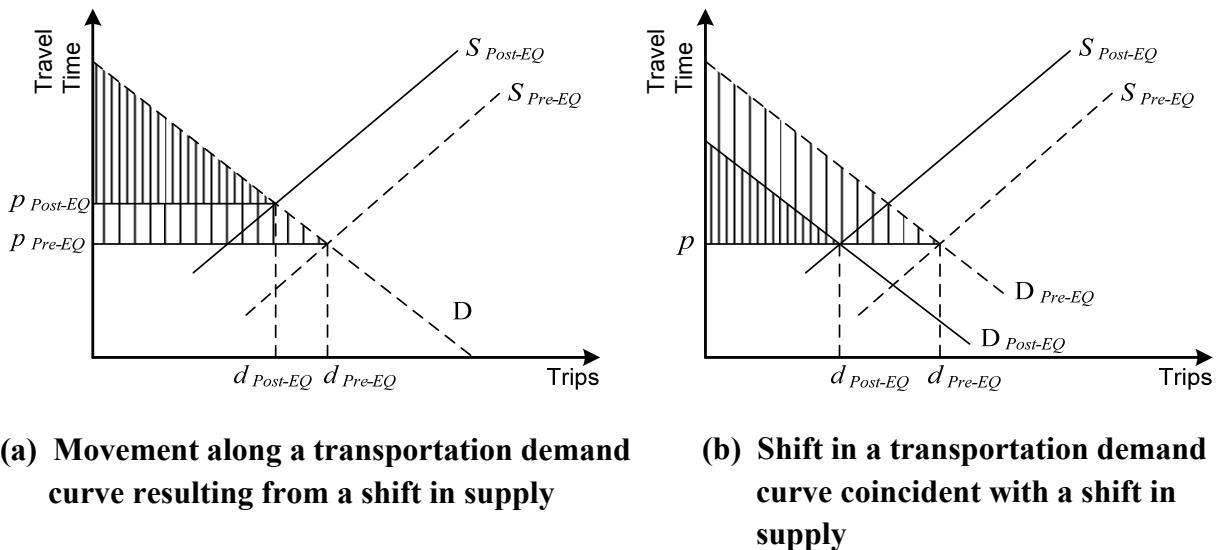


Fig. 6.1 Movement along demand curve versus shift in demand: Light hatched areas represent economic losses to remaining and absent travelers

One way to model a demand shift is via a detailed economic analysis of an urban activity system subject to an earthquake, but this is complex task generally beyond the scope and interests of transportation authorities. Instead, approximate conservative shifts in travel-demand curves might be imputed from more aggregate measures of damage to building stock. So long as these estimates are conservative, combining such a shift with approach described here would be a useful extension that would yield improved estimates of the value of forgone trips.

6.3 NETWORK DESIGN

Our work on assessment of economic losses provides the basic information needed to complete standard cost-benefit analyses with respect to allocating resources for disaster mitigation. Our long-term goal is to determine which mitigation projects should be undertaken. By retrofitting some subset of existing facilities, or by adding new components to a transportation network, system planners can change the post-earthquake network configuration. This changes network performance, and travelers' behavior. Broadly stated, our research goal is to find, subject to certain resource constraints, which components should be retrofitted, and where new components should be added so that the overall performance of any metropolitan transportation system is

most greatly improved. This well-defined network design problem is important in the transportation network literature (Yang and Bell 1998).

Individual users and network planners do not have the same objectives. Consequently, the network design problem often involves multiple levels of optimization. At the upper level, the system planner makes decisions on resource allocation to achieve the best system performance. At the lower level, the network users make their travel decisions based on their individual travel preferences. For a large network, this kind of network design problem is computationally challenging.

A post-earthquake network design problem is deterministic. The investigator is given a deterministic initial network condition to start with. This condition includes links damaged by an earthquake, and the investigator seeks to determine where and in what order link capacities should be added or restored subject to resource constraints. The standard objective function is aggregate network delay.

In contrast, in a pre-event network design problem, the occurrence and the scale of the damage and capacity loss resulting from seismic events in the planning period are uncertain. Therefore, the initial network configuration faced in the pre-event case is stochastic, and the optimal design problem becomes stochastic. This extra uncertainty makes the pre-event network design problem even more challenging. The problem has been formulated (Yang and Bell 1998) but never treated at a realistic scale. Subject to budget (and possibly other) constraints, the objective is to find the transportation network configuration on which user-equilibrium flows produce the minimum expected total congestion. This stochastic version of the problem is an embedded optimization problem with a tri-level structure. The upper level is the decision by the network authority, in this case a pre-event retrofit or reconstruction decision. The intermediate-level outcome, a function of the upper-level decision, is a random result of nature. The lower level, a function of the upper-level decision and the intermediate outcome, is the decision by the network user.

6.3.1 Design Problem Complexity

Assuming that retrofitting transportation structures is not a matter of degree but rather a binary decision, then a network with M transportation structures supporting its links presents 2^M retrofit

options. A random act of nature converts the network to a collection of $L < M$ links. The total number of possible networks to be considered is thus and an impossibly large value,

$$\sum_L^M C_L \cdot 2^L . \quad (6.1)$$

Explicit enumeration of options is out of the question. There are combinatorially times exponentially many retrofit options to be investigated, and no polynomial time algorithm available for identifying the best option among them for a given level of expenditures. Our work to date combines knowledge of seismic hazards, bridge fragilities, network performance, and traveler behavior to model the post-event performance of transportation networks. We do not have the means to evaluate all prospective post-event costs as the basis for pre-event mitigation decisions. However, useful progress is still possible.

6.3.2 Alternative Performance Metrics

Transportation network performance is typically measured by travel time, but other measures such as throughput and connectivity (Yang et al. 2000) are reasonable metrics for evaluation of the post-earthquake implications of pre-event mitigation decisions. A high level of reliability is an unstated given condition in most such applications. However, in a seismically damaged network, reliability provides a measure of the stability of the quality of service that the transportation system offers users. *Travel-time reliability* emphasizes on the probability that a trip between a given origin-destination pair can be made within a desired time interval. This reliability measure is relevant to assessing the quality of service of individual drivers' interest. Throughput reliability, also called *capacity reliability*, considers the probability that the network can successfully accommodate a certain level of travel demand. In general, capacity reliability is of more interest to transportation system managers. *Connectivity reliability* is concerned with the probability that a path exists between a given origin-destination pair. This definition of reliability is most essential in the context of emergency response after disaster, in particular, emergency vehicle routing.

If the system performance was measured only in terms of the connectivity of the network, then authorities would need to consider only the physical condition of the network rather than the level of service resulting from network-user interactions. This is a much simpler problem. However, if travel-time and capacity reliabilities are both of interest, then how would users

establish acceptability criteria for seismic losses from a seismic risk analysis? Because the solution space is so large, it is inevitable that heuristic approaches will be needed to study how to allocate given resources to improve the overall reliability of a transportation network subject to seismic risks and (by extension) other disasters. The reliability measure might include all three of the aforementioned definitions, but will require a departure from the standard network design perspective.

6.3.3 Role of Heuristics

Our work to date focuses on implementing efficient algorithms for network equilibrium analysis for large transportation networks. We have extended the standard application of these algorithms to account for how elevated delays suppress the demand for travel. The MCEER/FHWA REDARS project is unique in that it has focused on a probabilistic treatment of hazards and outcomes. The MCEER project is similar to research pursued by PEER researchers in that REDARS also suppresses representation of the urban economic activity system separate from the transportation systems.

It would certainly be feasible to use the REDARS tool configured for the Los Angeles or San Francisco Bay Area transportation network to investigate new heuristic approaches to network design. In particular, REDARS might be used to identify and evaluate simpler network design objectives than the minimization of total system delay and the economic value of trips forgone. These remain important metrics, but restricting attention to this standard objective locks investigators into an intractable mathematical programming problem.

Alternatively, investigators can take a game-theory approach to nature by applying game theory in the context of disaster mitigation. In this case, the system planner is a risk-averse player playing against nature. There are many possible earthquake events that nature could choose to play. There is a wide array of mitigation strategies that the system planner can choose to play. The planner assumes that the nature will do its best to destroy the system by picking possible combinations of earthquake events. Simultaneously, the planner will do his best to minimize losses by finding the best combination of possible strategies that he could play. This alternative approach to handling the uncertainty involved in nature requires relatively fewer assumptions about natural events and provides more risk-averse mitigation strategies, but also offers the advantage of tractability.

REFERENCES

- An, D., P. Gordon, J.E. Moore, II, and H.W. Richardson (2004) "Regional Economic Models for Performance Based Earthquake Engineering," *Natural Hazards Review* **5**(4), pp. 188-194.
- Caltrans, (3/1/1994). *Earthquake Detour Time Delay for March 1, 1994*, Traffic Management Branch.
- Office of Operations (Caltrans District 7) *Weekly Transportation Report* 1~15 (from Week of Feb 14 through July 8 1994), by Barton-Aschman Associates, Inc.
- (7/22/1994). *Northridge Earthquake Recovery – Intercept Survey of Trucks on Regional Travel Routes into Los Angeles*, Applied Management & Planning Group and Barton-Aschman Associates, Inc
- (9/6/1994). *Northridge Earthquake Recovery – Survey of Transit Riders on Metrolink Commuter Rail and Bus Routes*, NuStats Inc., and Barton-Ashman Associates Inc.
- (9/6/1994). *Northridge Earthquake Recovery – Home Interview Survey of Travelers Impacted by the Earthquake*, Applied Management and Planning Group, and Barton-Ashman Associates Inc.
- (11/17/1994). *Northridge Earthquake Recovery – Follow-up Home Interview Survey of Travelers Impacted by the Earthquake*, Applied Management and Planning Group, and Barton-Ashman Associates Inc.
- (9/8/1994). *Northridge Earthquake Recovery – Interim Transportation Report #1 for January 17 – March 31, 1994*, Barton-Ashman Associates Inc.
- (9/8/1994). *Northridge Earthquake Recovery – Interim Transportation Report #2 for April 1 – June 30, 1994*, Barton-Ashman Associates Inc.
- (9/15/1994). *Northridge Earthquake Recovery – Interstate 10 Recovery Report*, Barton-Ashman Associates Inc.
- (12/30/1994). *Northridge Earthquake Recovery – Interstate 5 / State Route 14 Recovery Report (January 17 – October 30, 1994)*, Barton-Ashman Associates Inc.
- (8/31/1995). *Northridge Earthquake Recovery – Final Comprehensive Transportation Analysis*, Barton-Ashman Associates Inc.
- Cho, S., P. Gordon, J. E. Moore, II, H.W. Richardson, M. Shinozuka, and S. Chang, (2001) "Integrating Transportation Network and Regional Economic Models to Estimate the Costs of a Large Earthquake," *Journal of Regional Science*, 41 (1), pp. 39-65.

- Cho, S., C.K. Huyck S. Ghosh S, and R.T. Eguchi (2003a) “A Validation Study of the Risks from Earthquake Damage to Roadway Systems (REDARS) Loss Estimation Software Program,” *Proceedings of 6th U.S. National Conference on Lifeline Earthquake Engineering*, Long Beach CA, August 10-13, 2003, pp. 878-885.
- Cho S., YY. Fan, and J.E. Moore, II (2003b) “Modeling Transportation Network Flows as a Simultaneous Function of Travel Demand, Earthquake Damage, and Network Level Service,” *Proceedings of 6th U.S. National Conference on Lifeline Earthquake Engineering*, Long Beach CA, August 10-13, 2003, pp. 868-877.
- Frank, M., and P. Wolfe (1956). An Algorithm for Quadratic Programming, *Naval Research Logistics Quarterly* 3 (1-2), pp. 95-110.
- Gordon, P., J.E. Moore, II, and R.W. Richardson (2002) Economic-Engineering Models for Earthquakes: Socioeconomic Impacts, PEER Report 2002/19, Berkeley, CA: Pacific Earthquake Engineering Research Center.
- Gordon, P and Q. Pan, (2001) *Assembling and Processing Freight Shipment Data: Developing a GIS-based Origin-Destination Matrix for Southern California Freight Flows*, National Center for Metropolitan Transportation Research (METTRANS) Project Report No. 99-25, University of Southern California, Los Angeles, CA.
- Kiremidjian, A., J. E. Moore, II, YY. Fan, N. Basoz, O. Yazali, and M. Williams (2006) *Pacific Earthquake Engineering Research Center Highway Demonstration Project*, PEER Report 2006/02, Berkeley, CA: Pacific Earthquake Engineering Research Center, forthcoming.
- LeBlanc, L. J., and K. Farhangian (1981). “Efficient Algorithms for Solving Elastic Demand Traffic Assignment Problems and Mode Split-Assignment Problems,” *Transportation Science* 15 (4), pp. 306-317.
- MCEER (9/2005). *REDARS 2.0 User Manual* (Draft), ImageCat Inc.
- (9/2005). *REDARS Import Wizard User Manual* (Draft), ImageCat Inc.
- (9/2005). *REDARS 2.0 Import Wizard Technical Manual* (Draft), Geodesy.
- Sheffi, Y. (1985). *Urban Transportation Networks*, Prentice-Hall, NJ.
- Taylor, C.E., S. D. Werner and S. Jakubowski (2001) “Walkthrough Method for Catastrophe Decision Making.” *Natural Hazards Review*, 2(4), pp. 193-202.
- Yang, H. and M.G.H. Bell (1998) “Models and Algorithms for Road Network Design: A Review and Some New Developments,” *Transportation Review* 18, pp. 257-278.

- Werner, S. D., S. Cho, C. E. Taylor, J. P. Lavoie, C. K. Huyck (2006) "Seismic Risk Analysis of a Roadway System in the Los Angeles, ," *Proceedings of the of the Fifth National Seismic Conference on Bridges and Highways*, San Francisco, September 18-20.
- Werner S.D., C.E. Taylor, S. Cho, J.P. Lavoie, C.K. Huyck, C. Eitzel, R.T. Eguchi, and J.E. Moore, II (2004) "New Developments in Seismic Risk Analysis of Highway Systems," *Proceedings of the 13th Annual World Conference on Earthquake Engineering*, Paper 2189, Vancouver, August 1-6, 2004.
- Werner S.D., C.E. Taylor, J.E. Moore, II, J.S. Walton, and S. Cho (2000) *A Risk-Based Methodology for Assessing the Seismic Performance of Highway Systems*, MCEER-00-0014. Buffalo, NY: Multidisciplinary Center for Earthquake Engineering Research.
- Yang H., K.K. Lo, and W.H. Tang (2000) "Travel Time Verses Capacity Reliability of a Road Network," *Reliability of Transportation Networks*, edited by M.G.H. Bell and C. Cassir C, Research Studies Press, ltd.: Baldock, Hertfordshire, England.

PEER REPORTS

PEER reports are available from the National Information Service for Earthquake Engineering (NISEE). To order PEER reports, please contact the Pacific Earthquake Engineering Research Center, 1301 South 46th Street, Richmond, California 94804-4698. Tel.: (510) 665-3405; Fax: (510) 665-3420.

- PEER 2006/09** *Quantifying Economic Losses from Travel Forgone Following a Large Metropolitan Earthquake.* James Moore, Sungbin Cho, Yue Yue Fan, and Stuart Werner. November 2006.
- PEER 2006/04** *Probabilistic Seismic Evaluation of Reinforced Concrete Structural Components and Systems.* Tae Hyung Lee and Khalid M. Mosalam. August 2006.
- PEER 2006/02** *Pacific Earthquake Engineering Research Center Highway Demonstration Project.* Anne Kiremidjian, James Moore, Yue Yue Fan, Nesrin Basoz, Ozgur Yazali, and Meredith Williams. April 2006.
- PEER 2006/01** *Bracing Berkeley. A Guide to Seismic Safety on the UC Berkeley Campus.* Mary C. Comerio, Stephen Tobriner, and Ariane Fehrenkamp. January 2006.
- PEER 2005/16** *Seismic Response and Reliability of Electrical Substation Equipment and Systems.* Junho Song, Armen Der Kiureghian, and Jerome L. Sackman. April 2006.
- PEER 2005/15** *CPT-Based Probabilistic Assessment of Seismic Soil Liquefaction Initiation.* R. E. S. Moss, R. B. Seed, R. E. Kayen, J. P. Stewart, and A. Der Kiureghian. April 2006.
- PEER 2005/14** *Workshop on Modeling of Nonlinear Cyclic Load-Deformation Behavior of Shallow Foundations.* Bruce L. Kutter, Geoffrey Martin, Tara Hutchinson, Chad Harden, Sivapalan Gajan, and Justin Phalen. March 2006.
- PEER 2005/13** *Stochastic Characterization and Decision Bases under Time-Dependent Aftershock Risk in Performance-Based Earthquake Engineering.* Gee Liek Yeo and C. Allin Cornell. July 2005.
- PEER 2005/12** *PEER Testbed Study on a Laboratory Building: Exercising Seismic Performance Assessment.* Mary C. Comerio, editor. November 2005.
- PEER 2005/11** *Van Nuys Hotel Building Testbed Report: Exercising Seismic Performance Assessment.* Helmut Krawinkler, editor. October 2005.
- PEER 2005/10** *First NEES/E-Defense Workshop on Collapse Simulation of Reinforced Concrete Building Structures.* September 2005.
- PEER 2005/09** *Test Applications of Advanced Seismic Assessment Guidelines.* Joe Maffei, Karl Telleen, Danya Mohr, William Holmes, and Yuki Nakayama. August 2006.
- PEER 2005/08** *Damage Accumulation in Lightly Confined Reinforced Concrete Bridge Columns.* R. Tyler Ranf, Jared M. Nelson, Zach Price, Marc O. Eberhard, and John F. Stanton. April 2006.
- PEER 2005/07** *Experimental and Analytical Studies on the Seismic Response of Freestanding and Anchored Laboratory Equipment.* Dimitrios Konstantinidis and Nicos Makris. January 2005.
- PEER 2005/06** *Global Collapse of Frame Structures under Seismic Excitations.* Luis F. Ibarra and Helmut Krawinkler. September 2005.
- PEER 2005/05** *Performance Characterization of Bench- and Shelf-Mounted Equipment.* Samit Ray Chaudhuri and Tara C. Hutchinson. May 2006.
- PEER 2005/04** *Numerical Modeling of the Nonlinear Cyclic Response of Shallow Foundations.* Chad Harden, Tara Hutchinson, Geoffrey R. Martin, and Bruce L. Kutter. August 2005.
- PEER 2005/03** *A Taxonomy of Building Components for Performance-Based Earthquake Engineering.* Keith A. Porter. September 2005.
- PEER 2005/02** *Fragility Basis for California Highway Overpass Bridge Seismic Decision Making.* Kevin R. Mackie and Bozidar Stojadinovic. June 2005.
- PEER 2005/01** *Empirical Characterization of Site Conditions on Strong Ground Motion.* Jonathan P. Stewart, Yoojoong Choi, and Robert W. Graves. June 2005.
- PEER 2004/09** *Electrical Substation Equipment Interaction: Experimental Rigid Conductor Studies.* Christopher Stearns and André Filiatrault. February 2005.

- PEER 2004/08** *Seismic Qualification and Fragility Testing of Line Break 550-kV Disconnect Switches.* Shakhzod M. Takhirov, Gregory L. Fenves, and Eric Fujisaki. January 2005.
- PEER 2004/07** *Ground Motions for Earthquake Simulator Qualification of Electrical Substation Equipment.* Shakhzod M. Takhirov, Gregory L. Fenves, Eric Fujisaki, and Don Clyde. January 2005.
- PEER 2004/06** *Performance-Based Regulation and Regulatory Regimes.* Peter J. May and Chris Koski. September 2004.
- PEER 2004/05** *Performance-Based Seismic Design Concepts and Implementation: Proceedings of an International Workshop.* Peter Fajfar and Helmut Krawinkler, editors. September 2004.
- PEER 2004/04** *Seismic Performance of an Instrumented Tilt-up Wall Building.* James C. Anderson and Vitelmo V. Bertero. July 2004.
- PEER 2004/03** *Evaluation and Application of Concrete Tilt-up Assessment Methodologies.* Timothy Graf and James O. Malley. October 2004.
- PEER 2004/02** *Analytical Investigations of New Methods for Reducing Residual Displacements of Reinforced Concrete Bridge Columns.* Junichi Sakai and Stephen A. Mahin. August 2004.
- PEER 2004/01** *Seismic Performance of Masonry Buildings and Design Implications.* Kerri Anne Taeko Tokoro, James C. Anderson, and Vitelmo V. Bertero. February 2004.
- PEER 2003/18** *Performance Models for Flexural Damage in Reinforced Concrete Columns.* Michael Berry and Marc Eberhard. August 2003.
- PEER 2003/17** *Predicting Earthquake Damage in Older Reinforced Concrete Beam-Column Joints.* Catherine Pagni and Laura Lowes. October 2004.
- PEER 2003/16** *Seismic Demands for Performance-Based Design of Bridges.* Kevin Mackie and Božidar Stojadinovic. August 2003.
- PEER 2003/15** *Seismic Demands for Nondeteriorating Frame Structures and Their Dependence on Ground Motions.* Ricardo Antonio Medina and Helmut Krawinkler. May 2004.
- PEER 2003/14** *Finite Element Reliability and Sensitivity Methods for Performance-Based Earthquake Engineering.* Terje Haukaas and Armen Der Kiureghian. April 2004.
- PEER 2003/13** *Effects of Connection Hysteretic Degradation on the Seismic Behavior of Steel Moment-Resisting Frames.* Janise E. Rodgers and Stephen A. Mahin. March 2004.
- PEER 2003/12** *Implementation Manual for the Seismic Protection of Laboratory Contents: Format and Case Studies.* William T. Holmes and Mary C. Comerio. October 2003.
- PEER 2003/11** *Fifth U.S.-Japan Workshop on Performance-Based Earthquake Engineering Methodology for Reinforced Concrete Building Structures.* February 2004.
- PEER 2003/10** *A Beam-Column Joint Model for Simulating the Earthquake Response of Reinforced Concrete Frames.* Laura N. Lowes, Nilanjan Mitra, and Arash Altoontash. February 2004.
- PEER 2003/09** *Sequencing Repairs after an Earthquake: An Economic Approach.* Marco Casari and Simon J. Wilkie. April 2004.
- PEER 2003/08** *A Technical Framework for Probability-Based Demand and Capacity Factor Design (DCFD) Seismic Formats.* Fatemeh Jalayer and C. Allin Cornell. November 2003.
- PEER 2003/07** *Uncertainty Specification and Propagation for Loss Estimation Using FOSM Methods.* Jack W. Baker and C. Allin Cornell. September 2003.
- PEER 2003/06** *Performance of Circular Reinforced Concrete Bridge Columns under Bidirectional Earthquake Loading.* Mahmoud M. Hachem, Stephen A. Mahin, and Jack P. Moehle. February 2003.
- PEER 2003/05** *Response Assessment for Building-Specific Loss Estimation.* Eduardo Miranda and Shahram Taghavi. September 2003.
- PEER 2003/04** *Experimental Assessment of Columns with Short Lap Splices Subjected to Cyclic Loads.* Murat Melek, John W. Wallace, and Joel Conte. April 2003.
- PEER 2003/03** *Probabilistic Response Assessment for Building-Specific Loss Estimation.* Eduardo Miranda and Hesameddin Aslani. September 2003.

- PEER 2003/02** *Software Framework for Collaborative Development of Nonlinear Dynamic Analysis Program.* Jun Peng and Kincho H. Law. September 2003.
- PEER 2003/01** *Shake Table Tests and Analytical Studies on the Gravity Load Collapse of Reinforced Concrete Frames.* Kenneth John Elwood and Jack P. Moehle. November 2003.
- PEER 2002/24** *Performance of Beam to Column Bridge Joints Subjected to a Large Velocity Pulse.* Natalie Gibson, André Filiatrault, and Scott A. Ashford. April 2002.
- PEER 2002/23** *Effects of Large Velocity Pulses on Reinforced Concrete Bridge Columns.* Greg L. Orozco and Scott A. Ashford. April 2002.
- PEER 2002/22** *Characterization of Large Velocity Pulses for Laboratory Testing.* Kenneth E. Cox and Scott A. Ashford. April 2002.
- PEER 2002/21** *Fourth U.S.-Japan Workshop on Performance-Based Earthquake Engineering Methodology for Reinforced Concrete Building Structures.* December 2002.
- PEER 2002/20** *Barriers to Adoption and Implementation of PBEE Innovations.* Peter J. May. August 2002.
- PEER 2002/19** *Economic-Engineered Integrated Models for Earthquakes: Socioeconomic Impacts.* Peter Gordon, James E. Moore II, and Harry W. Richardson. July 2002.
- PEER 2002/18** *Assessment of Reinforced Concrete Building Exterior Joints with Substandard Details.* Chris P. Pantelides, Jon Hansen, Justin Nadauld, and Lawrence D. Reaveley. May 2002.
- PEER 2002/17** *Structural Characterization and Seismic Response Analysis of a Highway Overcrossing Equipped with Elastomeric Bearings and Fluid Dampers: A Case Study.* Nicos Makris and Jian Zhang. November 2002.
- PEER 2002/16** *Estimation of Uncertainty in Geotechnical Properties for Performance-Based Earthquake Engineering.* Allen L. Jones, Steven L. Kramer, and Pedro Arduino. December 2002.
- PEER 2002/15** *Seismic Behavior of Bridge Columns Subjected to Various Loading Patterns.* Asadollah Esmaeily-Gh. and Yan Xiao. December 2002.
- PEER 2002/14** *Inelastic Seismic Response of Extended Pile Shaft Supported Bridge Structures.* T.C. Hutchinson, R.W. Boulanger, Y.H. Chai, and I.M. Idriss. December 2002.
- PEER 2002/13** *Probabilistic Models and Fragility Estimates for Bridge Components and Systems.* Paolo Gardoni, Armen Der Kiureghian, and Khalid M. Mosalam. June 2002.
- PEER 2002/12** *Effects of Fault Dip and Slip Rake on Near-Source Ground Motions: Why Chi-Chi Was a Relatively Mild M7.6 Earthquake.* Brad T. Aagaard, John F. Hall, and Thomas H. Heaton. December 2002.
- PEER 2002/11** *Analytical and Experimental Study of Fiber-Reinforced Strip Isolators.* James M. Kelly and Shakhzod M. Takhirov. September 2002.
- PEER 2002/10** *Centrifuge Modeling of Settlement and Lateral Spreading with Comparisons to Numerical Analyses.* Sivapalan Gajan and Bruce L. Kutter. January 2003.
- PEER 2002/09** *Documentation and Analysis of Field Case Histories of Seismic Compression during the 1994 Northridge, California, Earthquake.* Jonathan P. Stewart, Patrick M. Smith, Daniel H. Whang, and Jonathan D. Bray. October 2002.
- PEER 2002/08** *Component Testing, Stability Analysis and Characterization of Buckling-Restrained Unbonded Braces™.* Cameron Black, Nicos Makris, and Ian Aiken. September 2002.
- PEER 2002/07** *Seismic Performance of Pile-Wharf Connections.* Charles W. Roeder, Robert Graff, Jennifer Soderstrom, and Jun Han Yoo. December 2001.
- PEER 2002/06** *The Use of Benefit-Cost Analysis for Evaluation of Performance-Based Earthquake Engineering Decisions.* Richard O. Zerbe and Anthony Falit-Baiamonte. September 2001.
- PEER 2002/05** *Guidelines, Specifications, and Seismic Performance Characterization of Nonstructural Building Components and Equipment.* André Filiatrault, Constantin Christopoulos, and Christopher Stearns. September 2001.
- PEER 2002/04** *Consortium of Organizations for Strong-Motion Observation Systems and the Pacific Earthquake Engineering Research Center Lifelines Program: Invited Workshop on Archiving and Web Dissemination of Geotechnical Data, 4–5 October 2001.* September 2002.

- PEER 2002/03** *Investigation of Sensitivity of Building Loss Estimates to Major Uncertain Variables for the Van Nuys Testbed.* Keith A. Porter, James L. Beck, and Rustem V. Shaikhutdinov. August 2002.
- PEER 2002/02** *The Third U.S.-Japan Workshop on Performance-Based Earthquake Engineering Methodology for Reinforced Concrete Building Structures.* July 2002.
- PEER 2002/01** *Nonstructural Loss Estimation: The UC Berkeley Case Study.* Mary C. Comerio and John C. Stallmeyer. December 2001.
- PEER 2001/16** *Statistics of SDF-System Estimate of Roof Displacement for Pushover Analysis of Buildings.* Anil K. Chopra, Rakesh K. Goel, and Chatpan Chintanapakdee. December 2001.
- PEER 2001/15** *Damage to Bridges during the 2001 Nisqually Earthquake.* R. Tyler Ranf, Marc O. Eberhard, and Michael P. Berry. November 2001.
- PEER 2001/14** *Rocking Response of Equipment Anchored to a Base Foundation.* Nicos Makris and Cameron J. Black. September 2001.
- PEER 2001/13** *Modeling Soil Liquefaction Hazards for Performance-Based Earthquake Engineering.* Steven L. Kramer and Ahmed-W. Elgamal. February 2001.
- PEER 2001/12** *Development of Geotechnical Capabilities in OpenSees.* Boris Jeremi . September 2001.
- PEER 2001/11** *Analytical and Experimental Study of Fiber-Reinforced Elastomeric Isolators.* James M. Kelly and Shakhzod M. Takhirov. September 2001.
- PEER 2001/10** *Amplification Factors for Spectral Acceleration in Active Regions.* Jonathan P. Stewart, Andrew H. Liu, Yoojoong Choi, and Mehmet B. Baturay. December 2001.
- PEER 2001/09** *Ground Motion Evaluation Procedures for Performance-Based Design.* Jonathan P. Stewart, Shyh-Jeng Chiou, Jonathan D. Bray, Robert W. Graves, Paul G. Somerville, and Norman A. Abrahamson. September 2001.
- PEER 2001/08** *Experimental and Computational Evaluation of Reinforced Concrete Bridge Beam-Column Connections for Seismic Performance.* Clay J. Naito, Jack P. Moehle, and Khalid M. Mosalam. November 2001.
- PEER 2001/07** *The Rocking Spectrum and the Shortcomings of Design Guidelines.* Nicos Makris and Dimitrios Konstantinidis. August 2001.
- PEER 2001/06** *Development of an Electrical Substation Equipment Performance Database for Evaluation of Equipment Fragilities.* Thalia Agnanos. April 1999.
- PEER 2001/05** *Stiffness Analysis of Fiber-Reinforced Elastomeric Isolators.* Hsiang-Chuan Tsai and James M. Kelly. May 2001.
- PEER 2001/04** *Organizational and Societal Considerations for Performance-Based Earthquake Engineering.* Peter J. May. April 2001.
- PEER 2001/03** *A Modal Pushover Analysis Procedure to Estimate Seismic Demands for Buildings: Theory and Preliminary Evaluation.* Anil K. Chopra and Rakesh K. Goel. January 2001.
- PEER 2001/02** *Seismic Response Analysis of Highway Overcrossings Including Soil-Structure Interaction.* Jian Zhang and Nicos Makris. March 2001.
- PEER 2001/01** *Experimental Study of Large Seismic Steel Beam-to-Column Connections.* Egor P. Popov and Shakhzod M. Takhirov. November 2000.
- PEER 2000/10** *The Second U.S.-Japan Workshop on Performance-Based Earthquake Engineering Methodology for Reinforced Concrete Building Structures.* March 2000.
- PEER 2000/09** *Structural Engineering Reconnaissance of the August 17, 1999 Earthquake: Kocaeli (Izmit), Turkey.* Halil Sezen, Kenneth J. Elwood, Andrew S. Whittaker, Khalid Mosalam, John J. Wallace, and John F. Stanton. December 2000.
- PEER 2000/08** *Behavior of Reinforced Concrete Bridge Columns Having Varying Aspect Ratios and Varying Lengths of Confinement.* Anthony J. Calderone, Dawn E. Lehman, and Jack P. Moehle. January 2001.
- PEER 2000/07** *Cover-Plate and Flange-Plate Reinforced Steel Moment-Resisting Connections.* Taejin Kim, Andrew S. Whittaker, Amir S. Gilani, Vitelmo V. Bertero, and Shakhzod M. Takhirov. September 2000.
- PEER 2000/06** *Seismic Evaluation and Analysis of 230-kV Disconnect Switches.* Amir S. J. Gilani, Andrew S. Whittaker, Gregory L. Fenves, Chun-Hao Chen, Henry Ho, and Eric Fujisaki. July 2000.

- PEER 2000/05** *Performance-Based Evaluation of Exterior Reinforced Concrete Building Joints for Seismic Excitation.* Chandra Clyde, Chris P. Pantelides, and Lawrence D. Reaveley. July 2000.
- PEER 2000/04** *An Evaluation of Seismic Energy Demand: An Attenuation Approach.* Chung-Che Chou and Chia-Ming Uang. July 1999.
- PEER 2000/03** *Framing Earthquake Retrofitting Decisions: The Case of Hillside Homes in Los Angeles.* Detlof von Winterfeldt, Nels Roselund, and Alicia Kitsuse. March 2000.
- PEER 2000/02** *U.S.-Japan Workshop on the Effects of Near-Field Earthquake Shaking.* Andrew Whittaker, ed. July 2000.
- PEER 2000/01** *Further Studies on Seismic Interaction in Interconnected Electrical Substation Equipment.* Armen Der Kiureghian, Kee-Jeung Hong, and Jerome L. Sackman. November 1999.
- PEER 1999/14** *Seismic Evaluation and Retrofit of 230-kV Porcelain Transformer Bushings.* Amir S. Gilani, Andrew S. Whittaker, Gregory L. Fenves, and Eric Fujisaki. December 1999.
- PEER 1999/13** *Building Vulnerability Studies: Modeling and Evaluation of Tilt-up and Steel Reinforced Concrete Buildings.* John W. Wallace, Jonathan P. Stewart, and Andrew S. Whittaker, editors. December 1999.
- PEER 1999/12** *Rehabilitation of Nonductile RC Frame Building Using Encasement Plates and Energy-Dissipating Devices.* Mehrdad Sasani, Vitelmo V. Bertero, James C. Anderson. December 1999.
- PEER 1999/11** *Performance Evaluation Database for Concrete Bridge Components and Systems under Simulated Seismic Loads.* Yael D. Hose and Frieder Seible. November 1999.
- PEER 1999/10** *U.S.-Japan Workshop on Performance-Based Earthquake Engineering Methodology for Reinforced Concrete Building Structures.* December 1999.
- PEER 1999/09** *Performance Improvement of Long Period Building Structures Subjected to Severe Pulse-Type Ground Motions.* James C. Anderson, Vitelmo V. Bertero, and Raul Bertero. October 1999.
- PEER 1999/08** *Envelopes for Seismic Response Vectors.* Charles Menun and Armen Der Kiureghian. July 1999.
- PEER 1999/07** *Documentation of Strengths and Weaknesses of Current Computer Analysis Methods for Seismic Performance of Reinforced Concrete Members.* William F. Cofer. November 1999.
- PEER 1999/06** *Rocking Response and Overturning of Anchored Equipment under Seismic Excitations.* Nicos Makris and Jian Zhang. November 1999.
- PEER 1999/05** *Seismic Evaluation of 550 kV Porcelain Transformer Bushings.* Amir S. Gilani, Andrew S. Whittaker, Gregory L. Fenves, and Eric Fujisaki. October 1999.
- PEER 1999/04** *Adoption and Enforcement of Earthquake Risk-Reduction Measures.* Peter J. May, Raymond J. Burby, T. Jens Feeley, and Robert Wood.
- PEER 1999/03** *Task 3 Characterization of Site Response General Site Categories.* Adrian Rodriguez-Marek, Jonathan D. Bray, and Norman Abrahamson. February 1999.
- PEER 1999/02** *Capacity-Demand-Diagram Methods for Estimating Seismic Deformation of Inelastic Structures: SDF Systems.* Anil K. Chopra and Rakesh Goel. April 1999.
- PEER 1999/01** *Interaction in Interconnected Electrical Substation Equipment Subjected to Earthquake Ground Motions.* Armen Der Kiureghian, Jerome L. Sackman, and Kee-Jeung Hong. February 1999.
- PEER 1998/08** *Behavior and Failure Analysis of a Multiple-Frame Highway Bridge in the 1994 Northridge Earthquake.* Gregory L. Fenves and Michael Ellery. December 1998.
- PEER 1998/07** *Empirical Evaluation of Inertial Soil-Structure Interaction Effects.* Jonathan P. Stewart, Raymond B. Seed, and Gregory L. Fenves. November 1998.
- PEER 1998/06** *Effect of Damping Mechanisms on the Response of Seismic Isolated Structures.* Nicos Makris and Shih-Po Chang. November 1998.
- PEER 1998/05** *Rocking Response and Overturning of Equipment under Horizontal Pulse-Type Motions.* Nicos Makris and Yiannis Roussos. October 1998.
- PEER 1998/04** *Pacific Earthquake Engineering Research Invitational Workshop Proceedings, May 14-15, 1998: Defining the Links between Planning, Policy Analysis, Economics and Earthquake Engineering.* Mary Comerio and Peter Gordon. September 1998.

- PEER 1998/03** *Repair/Upgrade Procedures for Welded Beam to Column Connections.* James C. Anderson and Xiaojing Duan. May 1998.
- PEER 1998/02** *Seismic Evaluation of 196 kV Porcelain Transformer Bushings.* Amir S. Gilani, Juan W. Chavez, Gregory L. Fenves, and Andrew S. Whittaker. May 1998.
- PEER 1998/01** *Seismic Performance of Well-Confined Concrete Bridge Columns.* Dawn E. Lehman and Jack P. Moehle. December 2000.